Tunneling and Dynamics in Enzymatic Hydride Transfer

Zachary D. Nagel and Judith P. Klinman*

Department of Chemistry and Department of Molecular and Cell Biology, University of California, Berkeley, California 94720

Contents

1. Introduction

Enzymes continue to be the subject of intensive research efforts because of their ability to accelerate chemical reactions by factors as large as 10^{20} with extraordinary selectivity.[1] Despite enormous advances, on both experimental and theoretical fronts, our understanding of how proteins catalyze reactions remains incomplete. Biomimetic and engineered protein catalysts have failed to reach the catalytic efficiency of naturally occurring enzymes. In addition, computational methods continue to fall short of predicting with precision the catalytic properties of known structures, and the more ambitious goal of generating *de novo* enzymes with desired function. Evidently, the ultimate goal of using and engineering enzymes for biomedical and industrial applications still demands a deeper understanding of how the primary sequence of a protein determines its catalytic properties. This review is intended to provide insight into recent advances in the field of enzymology, with emphasis on experiments illuminating the role of protein dynamics from the richly informative perspective of hydride transfer.

1.1. Properties of Hydrogen and Protein Motion

A very large number of the known enzymatic reactions involve the transfer of hydrogen (where hydrogen can refer to a proton, hydrogen atom, or hydride). Because of the unique properties of the periodic table's lightest element, these reactions present at once a difficulty and an opportunity in terms of our understanding of biological catalysis: while hydrogen chemistry demands some special theoretical considerations, it also offers sensitivity of the reaction to environmental effects that can serve as a valuable probe of the subtle ways in which enzymes catalyze reactions.

1.1.1. Properties of Hydrogen

Several features distinguish hydrogen transfer from chemistry involving the exchange of bonds between heavier atoms.

* To whom correspondence should be addressed. Phone: (510) 642-2668. Fax: (510) 643-6232. E-mail: klinman@berkeley.edu.
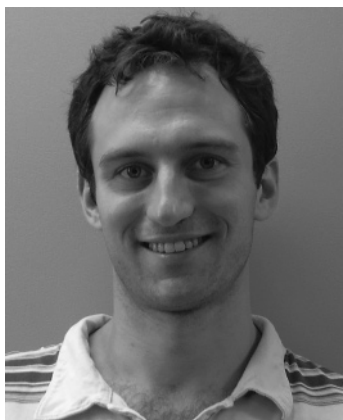
Zachary Nagel received his undergraduate degree in chemistry and biochemistry from the University of Michigan in 2003. Working under the direction of Charles Yocum, his undergraduate research focused on the role of Ca^{2+} in photosystem II. Zachary is now pursuing a Ph.D. at the University of California at Berkeley, working in Judith Klinman's lab. His graduate research concerns the role of tunneling and dynamics in the hydride transfer catalyzed by alcohol dehydrogenase, and the related question of how extremophilic enzymes adapt their structure and dynamics to achieve efficient catalysis at high and low temperatures.

Judith Klinman received her A.B. and Ph.D. degrees in chemistry from the University of Pennsylvania. She was a postdoctoral fellow at the Weizmann Institute of Science, Rehovot, Israel, and spent 10 years at the Institute for Cancer Research in Philadelphia, first as a postdoctoral fellow with Irwin Rose and later as a Staff Scientist. She has been on the faculty of the University of California, Berkeley, since 1978. Her research is currently focused on four areas: (i) nuclear tunneling in enzyme-catalyzed reactions and the relationship of this phenomenon to protein dynamics and the orgin of enzymatic rate accelerations; (ii) the mechanism of dioxygen activation by enzymes; (iii) the biogenesis and catalytic mechanism of quino-proteins and cofactors; and (iv) peroxide signaling in adipocytes. In addition to her lifelong fascination with enzymes, Dr. Klinman enjoys adventure travel, spending time with friends and family (especially her four grandchildren), and weekend retreats in Sonoma County.

First, because of its small mass, hydrogen has a de Broglie wavelength on the order of the distances over which it is expected to be transferred. It is, therefore, anticipated that quantum mechanical behavior will play a significant role in the chemical dynamics of hydrogen chemistry.[2] Second, there are three isotopes of hydrogen: protium, deuterium, and tritium with atomic mass 1, 2, and 3, respectively. Since the heavier isotopes will have the same chemical properties but significantly smaller de Broglie wavelengths, they can serve as a direct probe of quantum effects; this contrasts with electron transfer, where particles of variable mass are not available for kinetic studies.[3] Third, because the hydrogen donor and acceptor wave function overlap will be a very

sensitive function of the donor acceptor distance, environmental dynamics on a sub-angstrom scale can have a significant impact on the quantum mechanical aspects of hydrogen transfer.[4] Indeed, a picture is emerging wherein the quantum properties of hydrogen and the motions of enzymes are deeply connected in the mechanism of enzyme-catalyzed hydrogen transfer.

1.1.2. Protein Dynamics

Motion at the level of atoms and molecules is implicit in any reaction coordinate diagram; the energy varies as a function of bond angles, bond lengths, the distribution of charge, and the orientation and polarization of molecules. Without invoking protein dynamics explicitly, many proposals have been advanced to explain how enzymes can decrease the amount of thermal energy required to traverse the reaction coordinate, with the catalytic power of enzymes being intimately linked to a precisely defined structural relationship between the enzyme and substrate.[5,6] Though earlier theories of catalysis were largely focused on this structural (and static) aspect, it is also clear that any dynamical change in an enzyme has the potential to modify its interaction with its substrate and, hence, the efficiency of catalysis.

Accumulating experimental evidence suggests that protein motions can contribute significantly to function, including catalysis (cf. refs 7−10). Some of the initial evidence of a role for protein dynamics came from crystallographic studies of hemoglobin, which demonstrated a large conformational change upon the binding of oxygen.[11] Subsequent studies of enzymes in the presence and absence of substrate have indicated that substrate linked conformational changes are often critical for catalysis. Usually, such conformational changes represent the enzyme toggling between two states, one of which is inactive or much less active. In the simplifying case, where substrate binding does not contribute to the rate-determining step, this conformational change can be conceptualized as a thermodynamic effect that must reach equilibrium before the chemical step; that is, the process itself of going from the initial to final state has ended before the chemical step begins. In this manner, the dynamics of a protein conformational change can be temporally distinguished from protein dynamical effects that occur after formation of the E·S complex.

Once the E·S complex has formed, protein dynamics on a wide range of time scales (milliseconds to picoseconds) may occur and be coupled to catalysis. Protein dynamics can be very different from the molecular dynamics in water because of the covalent linkages and globular structure of proteins, which may be expected to affect both the amplitude and time scale of motions taking place. In principle, there are $3N - 6$ normal vibrational modes in a protein with N atoms (see the caveat below). These will have a wide range of force constants and frequencies corresponding to time scales measured in picoseconds for bond vibrations, nanoseconds for vibrations between globular regions, and microseconds for hinge bending motions such as that in maltose binding protein.[12] There are also rotational modes, for example, rotations of side chains that may take place on time scales ranging from nanoseconds to seconds, depending on the identity and environment of the side chain. The caveat to the $3N - 6$ rule is that in a solvent environment a large number of motions may be highly damped, so their motion cannot be described by a vibration. Instead, the motion represents a Markovian process dominated by thermal

fluctuations and frictional dissipation. Such motions are often invoked in discussions of functional nonequilibrium dynamics (cf. ref 13).

Allosteric transitions and local denaturation generally represent large-scale dynamical effects onto which the faster motions described immediately above may be superimposed. Although such bulk effects can usefully be treated as separate motions with their own time scales, these observable fluctuations are likely to represent the superposition of normal modes as opposed to the individual normal modes that are often used in computational studies. The motion of nonlinear substrates similarly involves $3N - 6$ vibrations [as well as rotations, and isomerizations, which may take place on the picosecond and femtosecond time scales (cf. the recent work on rhodopsin[14−16])].

1.1.3. Protein Motions Coupled to Catalysis

There are three broad categories into which motion may be placed with regard to its effect on catalysis. The first category is the trivial case where the motion is coincidental; that is, freezing out the motion of interest would have no effect on catalysis. In contrast, the motion may contribute to catalysis by modulating the potential energy landscape in such a way that freezing out the motion would slow the rate of catalysis. Within this context, the second and third categories (described below) are distinct in their time scale and directness of coupling to the reaction coordinate.

In the second category, enzyme (and possibly solvent) motion is part of the reaction coordinate; specific modes are coupled directly to the reaction coordinate in a way that enhances catalysis. A particular "rate-promoting vibration" is proposed to couple symmetrically to the reaction coordinate, thereby transferring the nonequilibrium character of some environmental modes. This is the framework used by Schwartz and co-workers and is reviewed in another paper in this thematic issue.[126]

In the third category, the environmental coordinates are not directly coupled to the reaction coordinate, but they still appear in a potential term in the Hamiltonian. Vibration along a mode that enhances the rate of the reaction is again proposed, but this mode is in thermal equilibrium with the bath and, therefore, assumes a probability (e.g. Boltzmann) distribution. The environmental motion is expected to occur on a time scale different from that of the observed chemical event, allowing the sampling of many protein configurations with a range of inherent reactivities; this is the type of motion most commonly invoked in hydrogen transfer reactions. Borrowing from the ideas advanced for molecular motors,[17] this landscape may be thought of as a kind of "track to the transition state," smoothing over local minima that could serve as potential sinks and increase the energy of activation for the comparable solution reaction.

An Arrhenius dependence would be observed in any of the three categories, and the catalytic effect can be thought of as a lowering of the phenomenological activation energy, E_a, as is assumed in the traditional theory of catalysis. But this picture increasingly seems oversimplified. When details that can be gleaned from careful kinetic experiments and theoretical studies are simply lumped into E_a, a failure to recognize key elements of design in biological catalysts can result. A growing body of experimental evidence suggests that it will be informative to scrutinize the motions that create the energy landscape traversed during the (catalyzed) reaction to see whether and how they contribute to the efficiency of
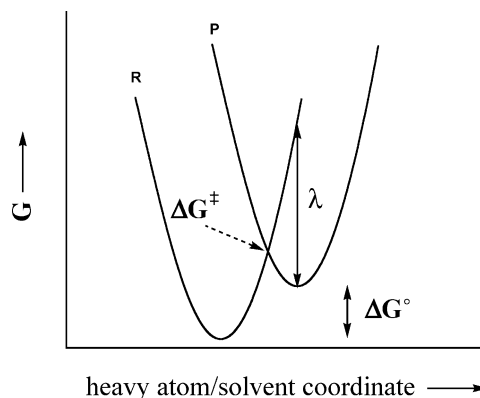

Figure 1. In the classical Marcus theory, the reactant and product potential surfaces are indicated by R and P, respectively, and their crossing point, $\Delta G^{\ddagger}$, represents the transition state with a free energy of activation defined in terms of λ and ΔG° (eq 1 in text).

the enzyme. To the extent that functionally important motions can be identified, they will represent an important engineering element in the *de novo* design of specialized enzymes. Experimental, theoretical, and computational evidence that motions play a role in catalysis is mounting and is presented within this paper in the context of the hydride transfer reactions catalyzed by alcohol dehydrogenases, dihydrofolate reductase, and glucose oxidase (sections 2, 3, and 4, respectively).

1.1.4. Reorganization and Preorganization

Even when motions are identified that are linked to catalysis, a conceptual (and ultimately detailed theoretical) framework is required to explain how the enzyme uses these motions to enhance the rate. To date, no rigorous and generally acceptable theory has been developed to describe such reactions, especially where light particles are involved and, in particular, for hydride transfer. To understand such catalysis fully, it will be necessary not only to improve this situation but also to distinguish the ways in which catalysis differs from unaided solution reactions. While the Marcus formalism discussed below does not solve this problem, it provides a useful framework for discussing a number of aspects of enzymatic catalysis.

It has been possible to extend the Marcus theory for electron transfer to describe other kinds of chemical reactions (cf. ref 18), and a number of enzyme systems have demonstrated kinetics consistent with this model. Equation 1 shows the simplest form of the Marcus equation in which the curvature for the reactant and product wells is the same and zero point energy levels have been omitted:[19]

$$k \propto \exp(-\Delta G^{\ddagger}/RT) = \exp\{-(\Delta G^{\circ} + \lambda)^2/(4\lambda RT)\} \quad (1)$$

According to the formalism, $\Delta G^{\ddagger}$ is the free energy of activation for the reaction, ΔG° is the driving force (on the enzyme), and λ is the reorganization energy. $\lambda/4$ is the energy needed to change the bond lengths, bond angles, molecular orientations, and polarization to the configuration that permits a reaction to occur at $\Delta G^{\circ} = 0$. It has been pointed out that λ can be reduced if the active site of the enzyme is already partially organized in a configuration close to the one it will adopt at the intersection of the two parabolas in Figure 1, which can be referred to as the transition state in this context. This idea has been expressed as part of the electrostatic basis for catalysis formulated by Warshel.[20] Some of the catalytic

effect derives from the fact that thermal energy is required to reorganize solvent molecules in the solution reaction, whereas the analogous process is not required on the enzyme because the active site is already structured in configurations that can stabilize the transition state.

In addition to the environmental reorganization term λ, that emerges from Marcus theory and determines the kinetic barrier for catalysis, the active site of an enzyme may undergo a preorganization that involves both the substrate and protein. A theoretical basis has been developed for substrate preorganization, defined as near attack conformers (NACs).[21] These define a family of preorganized substrate molecules as they become better positioned for catalysis on their way to the crossing point. In a similar manner, the protein backbone and side chains may be subject to considerable preorganization, leading to a subset of configurations that contain an optimal geometrical relationship of substrates in relation to one another and to the catalytically relevant functional groups within the active site. Importantly, it is anticipated that these preorganizations will be dynamical in nature, requiring considerable internal protein flexibility such that multiple configurations can be rapidly sampled. Conditions that impede such a sampling, as a result of, for example, mutagenesis of the protein or changes in temperature, will have the potential to seriously impede catalysis.

1.1.5. Adiabaticity and the Impact of Protein on Tunneling

For trajectories along the reaction coordinate that reach the intersection in Figure 1, a distinction is made between adiabatic reactions, where the electronic coupling between the product and reactant states is strong, and nonadiabatic reactions, where coupling is weak. This distinction has important consequences for the shape of the hydrogen potentials at the transition state.[22] In enzyme-catalyzed hydrogen atom transfers, where net neutral movement of the hydrogen nucleus has inherently less electronic coupling, it has been possible to formulate Marcus-like equations that permit a working separation of the tunneling process from the environmental motions that determine this process. By contrast, the more adiabatic nature of the movement of a charged particle (proton or hydride ion) makes such a separation of coordinates more problematic. Though a common conceptual approach is currently being used to describe the motions that contribute to catalysis for all three types of H-transfer ($H^\bullet$, H^+, and H^-), it is important to bear in mind that fundamental differences in the properties of charge transfer will influence the existing mathematical descriptions of the link between environmental motions and the efficiency of hydrogen wave function overlap.

One question that often arises in the context of H-transfer reactions is the extent to which an enzyme can increase the *fraction* of the reaction that proceeds via tunneling. Because of the properties of hydrogen discussed above, a far more reasonable approach begins with the assumption of quantum behavior and then examines the extent to which the structure and dynamics of the enzyme can facilitate the tunneling process. This facilitation is expected to be reflected in preorganization events involving substrate and enzyme, a possible reduction in λ, and a change in $\Delta G°$, as well as dynamical effects that allow a sampling of reduced distances between the hydrogen donor and acceptor (cf. eq 1 and Figure 7). We note that the framework described here can be extended to other reactions, and it represents a perspective on catalysis that goes beyond H-transfer (cf. the discussion

by Schwartz in another paper in this thematic issue[126]). The emerging ideas may also impact rational drug design where, especially in the context of H-transfer, it becomes impossible to define a "classical" transition state structure and, hence, an analogue of such a transition state; in these instances, an approach to the design of potent inhibitors could, in principle, involve interference with the enzyme's preorganization or reorganization dynamics that control the tunneling process.

1.1.6. Experimental Links of Protein Motion to Catalysis

The isolation and study of enzymatic H-transfer steps, in the context of protein structural and dynamical studies, affords an excellent approach to probe the link of protein motion to catalysis. Ideally, one would like to observe both tunneling and the protein dynamics directly. We note that *direct* observation of hydrogen tunneling is difficult because the tunneling takes place between bound states. In the case of a decaying nucleus, it was possible to show the *escape* of an α particle by tunneling through the potential barrier as a result of a measurable kinetic energy that was less than the classically expected value.[2] For reactions in solution, it is often possible to study hydrogen transfer down to very low temperatures, allowing an activationless tunneling region to be observed directly. However, the limited temperature ranges available for the study of most enzymatic reactions precludes this approach. One of the simplest ways to impede tunneling is to increase the mass of the transferred particle, namely by substituting deuterium or tritium for protium in the reaction. In fact, the impact of isotopic substitution on kinetic behavior has provided some of the most robust evidence for nonclassical behavior in enzyme (cf. refs 23–25 for an introduction to and review of these approaches).

Motions that take place on time and distance scales in the ranges of a nanosecond and an angstrom may be important for tunneling, but these are difficult to detect experimentally.[26,27] Whereas slower motions in proteins may be more readily experimentally accessible, it is the link of this motion to catalysis that is of greatest relevance. In general, the role of enzyme motion is probed by looking for *correlations* between a modulation in protein dynamics and its impact on catalysis. This can be achieved by, for example, site-directed mutagenesis, by variation in temperature (to shift the population of activated protein modes), and by examination of a family of homologous proteins that function within different temperature niches. As will be discussed in section 2, a thermophilic alcohol dehydrogenase has afforded a unique opportunity to observe a "switch" in protein flexibility that affects tunneling behavior. With regard to site-specific mutagenesis, studies of dihydrofolate reductase (described in section 3) indicate how it is possible to disrupt dynamics, or decouple the effects of dynamics from catalysis, by mutating amino acids that are distal to the active site. In all of these studies, some of the strongest experimental evidence of a role for dynamics in catalysis has come from kinetic hydrogen isotope effects and their attendant properties: Because of the extreme sensitivity of quantum tunneling to environmental effects, hydrogen transfer reactions offer an excellent experimental system in which to probe dynamics in enzyme reactions.

2. Alcohol Dehydrogenases

Some of the very earliest investigations of the mechanistic principles that underlie enzyme catalysis were focused on

the class of proteins that use the nicotinamide cofactors, NAD^+ and $NADP^+$. These dehydrogenases catalyze the net transfer of a hydride ion from a substrate donor to a cofactor in a stereospecific manner.[28,29] X-ray studies of numerous members of this class of enzyme have indicated separate domains for substrate and cofactor binding, with the cofactor domain being constructed from a conserved, Rossmann fold.[30] During the past decade and a half, studies of the alcohol dehydrogenases have played a very significant role in moving us beyond a classical and static view of enzyme catalysis toward one that embraces hydrogen tunneling and its intimate link to the dynamical features of proteins.

2.1. Yeast and Horse Liver Alcohol Dehydrogenase

2.1.1. Probes of Tunneling

Classical steady-state kinetic studies of these enzymes had shown that under conditions of substrate saturation the rate of enzyme turnover was controlled by the release of bound cofactor, with cofactor binding being linked to conformational changes that are a prerequisite for effective chemical catalysis (cf. ref 31). Numerous tools have been introduced to study the detailed chemistry of the hydride transfer step, including single turnover kinetics and the extensive use of kinetic isotope effects. Among the first applications of kinetic isotope effects was a study of the reduction of acetaldehyde by protonated (NADH) and deuterated (NADD) cofactor catalyzed by horse liver alcohol dehydrogenase (HLADH), showing that the magnitude of the primary isotope effect (see below for definition) decreased from 2.7 to unity as the concentration of aldehyde was increased from sub-saturating to saturating levels.[32] This was subsequently shown to arise from a "switch-over" from the measurement of a second-order rate constant, k_{cat}/K_m, under conditions of low aldehyde concentration, to k_{cat} at saturating substrate. These experiments led to the recognition that the k_{cat}/K_m parameter can be used to characterize the hydride transfer step under steady state conditions. This approach has become a particularly useful one when the acetaldehyde/ethanol pair is substituted by slower substrates, ensuring that chemistry controls the measured k_{cat}/K_m parameter.[33-35]

The first intimation of tunneling in the ADH reaction came from two surprising observations in the measurement of primary and secondary isotope effects in the alcohol oxidation direction (eq 2):

(2)
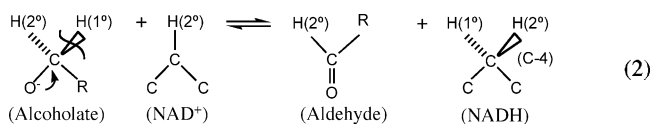
where the primary isotope effect refers to the hydride ion transferred between substrate and cofactor and the secondary isotope effect refers to the hydrogen that remains in the product(s).

First, using cofactor that had been labeled with deuterium at the C-4 position of the nicotinamide ring, a kinetic secondary isotope effect was measured that exceeded the value measured under equilibrium conditions.[36] Up to that point it had been assumed that the equilibrium, $sp^2 \rightleftharpoons sp^3$ interconversion at the cofactor would provide an upper limit for kinetic isotope effects. Second, when the impact of isotopic substitution at the primary and secondary positions of the alcohol was interrogated, different conclusions regard-

ing transition state structures were reached, with the primary isotope effect implicating a symmetrical transition state and the secondary isotope effect a late transition state.[37] Both of these findings caused considerable debate, ultimately leading to the proposal of a nuclear tunneling component to the hydride transfer from donor to acceptor.

A test of this provocative hypothesis was undertaken in the YADH reaction, using as substrate benzyl alcohol that had been labeled with either protium and tritium or deuterium and tritium at the C-1 position, with the former providing k_H/k_T and the latter providing k_D/k_T. Because of the method of labeling and measurement, the isotope effects were on k_{cat}/K_m, circumventing any complication from rate-limiting cofactor release.[38]

(3)

(4)
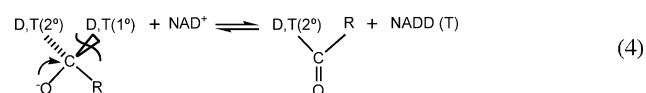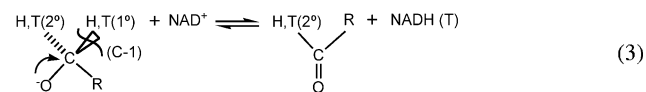
The magnitude of measured k_H/k_T values was found to be consistent with previous values for k_H/k_D, in particular indicating a secondary k_H/k_T at the equilibrium limit and a primary k_H/k_T consistent with hydride transfer being fully rate-determining. In the case of the primary k_D/k_T, this was found to be somewhat suppressed for the primary, transferred hydrogen and very significantly reduced for the secondary position.[38]

The interconnection among rate constants for the three isotopes of hydrogen has been named the Swain–Schaad relationship and is written as shown in eq 5 for k_D/k_T and k_H/k_T:

$$(k_D/k_T)^{EXP} = k_H/k_T \quad (5)$$

$$EXP = \ln(k_H/k_T)/\ln(k_D/k_T) \quad (6)$$

where the exponent arises from zero point energy differences among H, D, and T and a semiclassical treatment of the isotope effect. In simple models, the value for EXP is predicted to be ca. 3.26;[39] several investigators have questioned the upper limit for EXP in the absence of tunneling, finding that, for measured values of $k_H/k_T \geq 1.1$, a more conservative upper limit for the exponent is 4–5.[40,41] Prior to the experimental measurements, it had been proposed that a greater tunneling contribution to the transfer of H than D might be expected to elevate k_H/k_T in relation to k_D/k_T, inflating the exponent in eq 6 above 3.26; it was further proposed that motional coupling between the primary and secondary hydrogens would produce an aberrant relationship among the secondary isotope effects.[42]

The experimentally observed value of $10(\pm 2)$ for the exponent relating the secondary isotope effects in the YADH reaction[38] immediately confirmed a breakdown in the rule of the geometric mean (which predicts that the secondary isotope effect will be independent of the mass transferred in the primary position) and provided the first definitive evidence for nonclassical behavior during an enzyme catalyzed C–H activation process. At the time of publication, the data were attributed to a tunneling "correction" in which tritium (atomic mass of 3) tunnels very little while protium tunnels more than deuterium, inflating k_H/k_T in relation to

k_D/k_T. Though it was not clear why the deviation from eq 6 was restricted to the secondary position, it was thought that this reflected the smaller value of the secondary isotope effect and its enhanced sensitivity to deviations from the semiclassical limit.

In light of the availability of extensive structural data for the homologous horse liver alcohol dehydrogenase (HLADH), together with the lack of an X-ray structure for YADH, the study of the relationship of k_H/k_T to k_D/k_T was extended to the HLADH system,[44] with the goal of relating tunneling behavior to active site structure. Using the unnatural substrate (benzyl alcohol) and wild-type enzyme, the magnitude of the exponent, eq 6, for secondary kinetic isotope effects was in fact found to lie close to its semiclassical value. Since earlier calculations had predicted that kinetic complexity (i.e., the contribution of steps other than hydride transfer to the measured parameter) could *reduce* the magnitude of the exponent,[38] the smaller value for the exponent in the HLADH reaction was attributed to hydride transfer being only partially rate-determining. Two active site mutants were introduced near the substrate-binding pocket, Leu[57] $\rightarrow$ Phe and Phe[93] $\rightarrow$ Trp, with the intention of introducing steric crowding to the bound substrate and increasing its dissociation rate from the ternary complex of enzyme, NAD^+, and benzyl alcohol. As anticipated, the magnitude of the exponent for both mutants became elevated near to that for YADH, and site-specific mutagenesis was concluded to have "unmasked tunneling" in the HLADH reaction.[44]

2.1.2. Role of Valine 203 in HLADH

One feature of all dehydrogenases is the presence of a bulky hydrophobic residue that resides behind the bound nicotinamide ring, ensuring a close approach between the reactive C-4 of the cofactor and C-1 of the alcohol. In HLADH, a series of site-specific mutagenesis studies has been carried out to examine the impact of the reduction in size of this residue on both catalytic efficiency and the size of the exponent relating k_D/k_T to k_H/k_T. An X-ray structure of the V203A mutant of HLADH has shown that the nicotinamide ring of bound cofactor has moved away from C-1 of a substrate analogue, trifluoroethanol, by ca. 0.8 Å (Figure 2) concomitant with a reduction in k_{cat}/K_m of ca. 100-fold.[35] In independent studies, Plapp and co-workers showed a reduction in the unimolecular rate constant for hydride transfer from bound alcohol to NAD^+ of ca. 16-fold in V203A.[45] This theme, of a role for active site hydrophobic side chains in maintaining optimal positioning between the hydrogen donor and acceptor, has been seen as well in the hydrogen atom transfer catalyzed by the enzyme lipoxygenase.[4]

The impact of the mutagenesis at position 203 on the exponent (cf. eq 6) representing the secondary isotope effects was also examined, indicating a regular trend in which the size of the exponent decreased as the size of the residue at position 203 decreased (Figure 3).[35] This was interpreted, once again, in the context of a tunneling "correction", with the implication that a relaxation in the distance between the hydrogen donor and the acceptor had diminished the contribution of tunneling to the observed rate. Table 1 summarizes the observed values of the α-secondary k_H/k_T and k_D/k_T for both YADH, using a series of benzyl alcohol substrates, and HLADH, using a series of site-specific mutants. A dominant feature of these data is the variability of the value of EXP under a range of experimental condi-
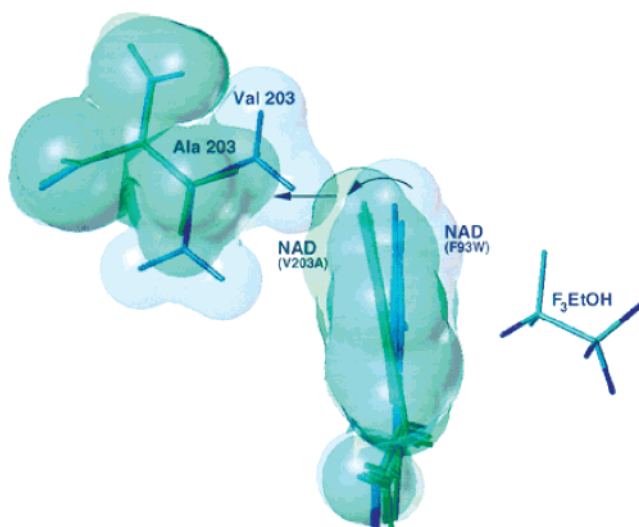

Figure 2. Comparison of the configuration of NAD^+ based on X-ray structures of abortive complexes for mutants of HLADH with bound cofactor and trifluoroethanol. Upon expansion of the active site, V203A, the nicotinamide ring tilts away from the active site. Reproduced with permission from ref 35. Copyright 1997 National Academy of Sciences, U.S.A.
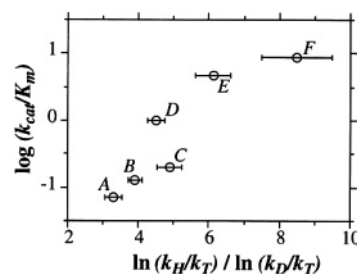
Figure 3. Relationship between the log of the bimolecular rate constant and the exponent (EXP in eq 6 in the text): (A) V203G; (B) V203A:F93W; (C) V203A; (D) V203L; (E) F93W; (F) L57F. Reproduced with permission from ref 35. Copyright 1997 National Academy of Sciences, U.S.A.

tions. Surprisingly, the trend in the exponent is mirrored by the change in k_D/k_T, with the aggregate data indicating a constant value for $k_H/k_T = 1.34$ (0.01).[3] This is in contrast to a tunneling "correction" model, where changes in conditions would be expected to alter k_H/k_T, the parameter most sensitive to the tunneling probability. This unexpected behavior of the secondary isotope effects is discussed further in section 2.3.

2.1.3. Low Temperature Behavior

The impact of site-specific mutagenesis studies described above shows, at a minimum, a static contribution of an active site residue in maintaining the correct geometry between the hydrogen donor and acceptor for efficient H-transfer. However, even when the distance between donor and acceptor is at van der Waals contact in the Michaelis complex, further distance reduction is expected to be necessary for efficient tunneling, implicating the contribution of active site motions to the reaction coordinate.

It was reasoned that a reduction in the temperature of the enzyme reaction substantially below 0 °C might be expected to reduce active site motions, providing an experimental link between such motions and tunneling. However, when competitive and noncompetitive primary and secondary isotope effects were measured down to −50 °C using WT-

Table 1. Variation in the Exponent Relating the Secondary H/T and D/T Isotope Effects in Response to Changes in Substrate or Protein Structure

enzyme[a]	$\alpha-2° \, k_H/k_T$[b]	$\alpha-2° \, k_D/k_T$[b]	EXP[c]	ref
YADH, WT (p-H)[d]	1.35 (0.015)	1.03 (0.006)	10.2 (2.4)	38
YADH, WT (p-Cl)[d]	1.34 (0.01)	1.03 (0.010)	9.9 (4.2)	115
HLADH, L57F	1.318 (0.007)	1.033 (0.004)	8.5 (1)	44
HLADH, F93W	1.333 (0.004)	1.048 (0.004)	6.3 (0.5)	44
HLADH, V203A	1.316 (0.006)	1.058 (0.004)	4.9 (0.3)	35
HLADH, L57V	1.332 (0.003)	1.065 (0.011)	4.55 (0.75)	44
HLADH, V203L	1.38 (0.005)	1.074 (0.004)	4.5 (0.2)	35
HLADH, WT[e]	1.335 (0.003)	1.073 (0.008)	4.1 (0.44)	44
HLADH, ESE[e]	1.332 (0.004)	1.075 (0.003)	3.96 ((0.16)	44
HLADH, V203A:F93W	1.325 (0.004)	1.075 (0.004)	3.9 (0.2)	35
HLADH, V203G	1.358 ((0.007)	1.097 (0.007)	3.3 (0.2)	35
YADH WT (p-MeO)[d]	1.34 (0.04)	1.12 (0.02)	2.78 (0.82)	123

[a] HLADH is horse liver alcohol dehydrogenase, and YADH is yeast alcohol dehydrogenase. [b] Reported values ± the standard errors. [c] The error was calculated as follows: error $= \exp[\{\delta \, \ln(k_H/k_T)/\ln(k_H/k_T)\}^2 + \{\delta \, \ln(k_D/k_T)/\ln(k_D/k_T)\}^2]^{1/2}$. [d] These experiments used benzyl alcohols with either H, Cl, or MeO substituents in the *para*-position of the ring. [e] H-transfer may not be fully rate-determining for these two enzyme forms, leading to a somewhat reduced value for EXP.

HLADH, both the isotope effects and their exponential relationships were found to decrease.[46] These results were in the direction expected for increasing kinetic complexity at reduced temperatures, indicating that the WT enzyme was unsuitable for such studies.

Given the earlier conclusion that the F93W mutant of HLADH could facilitate the analysis of tunneling by reducing kinetic complexity at room temperature, studies were pursued with this mutant in water/methanol mixtures down to −30 °C (the stability of F93W precluded analysis at lower temperatures).[46] In noncompetitive studies, the isotope effect on k_{cat}/K_m(alcohol) showed a regular increase with decreasing temperature (from 3.5 to 7.5), indicating a temperature dependence for the isotope effect that was greater than that expected based on semiclassical theory, $A_H/A_D = 0.015$ (0.013), where, for semiclassical behavior, $k_H/k_D \leq 7$ and $0.7 < A_H/A_D < 1.2$ (Table 2):

$$\frac{k_H}{k_D} = \frac{A_H}{A_D} \exp\left(\frac{E_a(D) - E_a(H)}{RT}\right) \qquad (7)$$

In competitive measurements, there also appeared to be an enhanced temperature dependence of the primary H/T and D/T isotope effects, though this was less dramatic than that observed for the H/D experiment, $A_H/A_T = 0.33$ (0.16) (the semiclassical limit is 0.6, Table 2). These can be compared to the results from temperature-dependent studies of H/T for F93W in water at the elevated temperature range from 0 to 45 °C, where $A_H/A_T = 0.49(0.05)$. It is difficult to conclude with certainty that there is any statistically significant difference between the behavior of HLADH above 0 °C (in water) and below 0 °C (in methanol/water mixtures). At most, there is a slightly greater deviation from classical expectations at the reduced temperature, which is what would be anticipated for simple chemical reactions where tunneling increases as the temperature is decreased.[2]

Table 2. Estimated Range for $A_{(light)}/A_{(heavy)}$ in the Semiclassical Limit[a]

ratio	semiclassical range
A_H/A_D	0.7−1.2
A_H/A_T	0.6−1.3
A_D/A_T	0.9−1.1

[a] Reference 124.

Turning to the exponential relationship between the secondary k_H/k_T and k_D/k_T at reduced temperatures, this was found to be 5.7(1.3) from the average of two values at 3 °C in 40 and 60% methanol. As the temperature was lowered below 0 °C, an average value of 7.6(0.4) could be calculated (eliminating the outlier at −30 °C). Once again, if we return to the behavior of HLADH at room temperature, exponents of 6.3(0.5) and 8.5(1) were measured for F93W and L57F, respectively;[35] these two mutant forms have been used interchangeably to examine hydride transfer parameters in the absence of kinetic complexity. Once again, as with kinetic isotope effects measured at the primary position, there does not appear to be a very significant difference in behavior above and below 0 °C regarding the magnitude of the exponent, though this may be increasing somewhat at the reduced temperatures.

It must be concluded that these technically demanding experiments were not, in the end, very informative regarding the possible link of protein motions to catalysis. In actuality, the behavior of the hydride transfer step did not change very substantially at reduced temperatures. This could indicate that the natural tendency for tunneling to increase at low temperature had been offset by a decrease in key protein motions. A more likely explanation is that motions that are contributing to the measured properties of the hydride transfer are quite rapid (possibly on the nanosecond to picosecond time scale) and local, such that a reduction in temperature to −30 °C was simply insufficient to freeze out the relevant motions.

2.2. Prokaryotic Alcohol Dehydrogenases

In recent years, a class of tetrameric prokaryotic alcohol dehydrogenases has been described that contains proteins that are very similar with regard to both their primary sequences and their three-dimensional structures.[47−49] This class of enzymes includes a psychrophilic variant from *Moraxella* TAE123 (ps-ADH) that functions optimally at 5 °C,[50] a mesophilic variant from *E. coli* (ec-ADH),[47] and a high-temperature ADH from *B. stearothermophilus* (ht-ADH) that functions up to 65 °C.[49] The different temperature niches under which these proteins function introduce the possibility of examining the experimental link between protein stability/ flexibility and the efficiency of hydride transfer.

2.2.1. High Temperature Alcohol Dehydrogenase (ht-ADH)

Steady-state kinetic studies of ht-ADH using NAD^+ and benzyl alcohol have revealed a transition in the Arrhenius behavior at ca. 30 °C, from a reaction with a relatively small enthalpy of activation above the break temperature ($E_a = 13.9$ kcal/mol) to a more sluggish reaction with $E_a = 20.6$ kcal/mol below 30 °C.[51] Furthermore, the break in behavior is more exaggerated for oxidation of deuterated benzyl alcohol, with the consequence that the isotope effect changes from being close to temperature-independent above 30 °C to strongly temperature-dependent below 30 °C. In experiments with other enzymes, it has been shown that perturbation away from optimal reaction conditions produces an increasing temperature dependence for the isotope effect, where the perturbing condition has been either the use of a less efficient substrate or a change in a protein active site side chain via site-specific mutagenesis (cf. refs 4, 52, and 53). The data with ht-ADH provided the first evidence for induction of an increase in the temperature dependence of the isotope effect through a change in reaction temperature.

In conjunction with noncompetitive isotope effects, which focused on comparative k_{cat} values for protium vs deuterium, extensive competitive isotope effects (on k_{cat}/K_m) have also been measured with ht-ADH. [51] The temperature dependence of H/T and D/T shows patterns similar to that of H/D, i.e., close to temperature-independent isotope effects above 30 °C, converting to temperature-dependent effects below 30 °C (Table 3). The availability of both D/T and H/T allowed

Table 3. Temperature Dependence of the Swain−Schaad Exponent and Isotopic Arrhenius Prefactors for ht-ADH[a]

temp range	A_H/A_D	A_H/A_T	A_D/A_T	EXP
5−30 °C	1×10^{-5} (1×10^{-5})	0.26 (0.23)	0.23 (0.14)	6.12 (0.80)[b]
30−65 °C	2.2 (1.1)	4.3 (0.6)	1.73 (0.26)	12.6 (1.52)[b]

[a] Reference 52. [b] These are average values from within the stated temperature ranges.

a calculation of their interrelationship, according to eq 6. As seen previously with YADH and HLADH, the value of the exponent was inflated for the secondary isotope effect, with an average value of 6.1 below 30 °C, increasing to an average value of 12.6 above the break point (Table 3). A persistent challenge has been to relate deviations from semiclassical Swain−Schaad predictions to deviations from semiclassical temperature dependencies of the isotope effect. This will be addressed in section 2.3.

Keeping in mind that the ht-ADH is designed to function at high temperature, it might be expected that its altered behavior below 30 °C is a result of the enzyme having become too rigid to function efficiently as a catalyst. In an experiment that measured global hydrogen/deuterium exchange from solvent into the peptide backbone of native state ht-ADH vs YADH, it was found that the flexibility of the YADH at room temperature matched that of the ht-ADH at the elevated temperature (above 30 °C), with the global exchange of ht-ADH below 30 °C pointing toward an overall more rigid protein.[54]

Coupling H/D exchange to limited proteolysis of the exchanged protein, and characterization of the resulting peptides (21 peptides that correspond to ca. 95% of the protein sequence) by mass spectrometry, enabled local assignment of changes in flexibility within the native protein.[55] The analysis of the (pH 7) exchange behavior was based on a two-state model (designated EX-2)[56,57] that involves a rapid and transient opening of the protein to expose a set of amide linkages to solvent, $K_{(open)}$, followed by a rate-limiting chemical exchange process, $k_{(cxch)}$:

$$k_{(EX-2)} \sim K_{(open)} k_{(exch)} \tag{8}$$

Eleven of the analyzed peptides showed a regular increase in the rate of deuterium incorporation between 10 and 65 °C,[55] compatible with the expected temperature dependence of both $K_{(open)}$, which describes a rare event and is expected to have a positive $\Delta H°$, and $k_{(exch)}$, which has been reported to have a $\Delta H^‡$ of ca. 17 kcal/mol.[58] Five of the remaining peptides showed very little change in their exchange behavior up to ca. 45 °C, with a pattern above this temperature indicative of increased exchange.[55] This transition was found to correspond to a change in the K_d for the cofactor, as measured by fluorescence titration, suggesting an interconversion between enzyme forms with the combined properties of different flexibilities and cofactor binding (eq 9):

$$\tag{9}$$
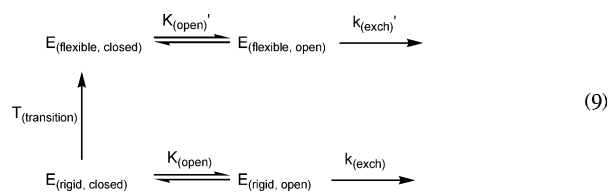
where $K_{(open)} < K_{(open)}'$.

In the context of eq 9, a particularly interesting set of observations was made for the remaining five peptides, which also indicated a temperature transition in exchange behavior. In this latter case, the $T_{(transition)}$ was observed at 30 °C (Figure 4), *the same temperature previously shown to alter both the enthalpy of activation for ht-ADH and the temperature dependence of its kinetic isotope effects.*[51,55]

The 10 peptides that show a $T_{(transition)}$, eq 9, could be correlated with the three-dimensional protein structure. Using the recently determined X-ray structure of the ht-ADH[49] (Figure 5), the results indicated that the two observed transitions in flexibility are local and largely confined either to the cofactor-binding domain ($T_{(transition)} \sim 45$ °C) or to the substrate-binding domain ($T_{(transition)} \sim 30$ °C).[55] We believe that both of these transitions, which reflect increased mobility in the protein, are enhancing catalysis, with the transition at 30 °C having the greatest impact on the rate constant for hydride transfer and its attendant properties. One important feature of the data is the 30 °C transition that occurs in a region of a protein that is outside the tetramerization domain and, hence, is not expected to reflect any change in intersubunit interactions as the temperature is altered.[49]

The H/D exchange of a protein measured using limited proteolysis/mass spectrometry can permit an analysis of the dynamical properties of a protein that is too large for analysis by NMR. However, the resolution using mass spectrometry is inherently less than that for NMR, since one is measuring the average properties of a peptide (typical length of 10 amino acids) rather than individual amino acids. Nonetheless, the data collected for ht-ADH show that among the five peptides whose $T_{(transition)}$ corresponds to the temperature transition for a change in hydride/tunneling properties, four peptides have loops that are in position to contact the bound substrate (or substrate analogue, trifluoroethanol, in the X-ray structure). We have concluded that these data provide some of the most direct experimental evidence of a role for local
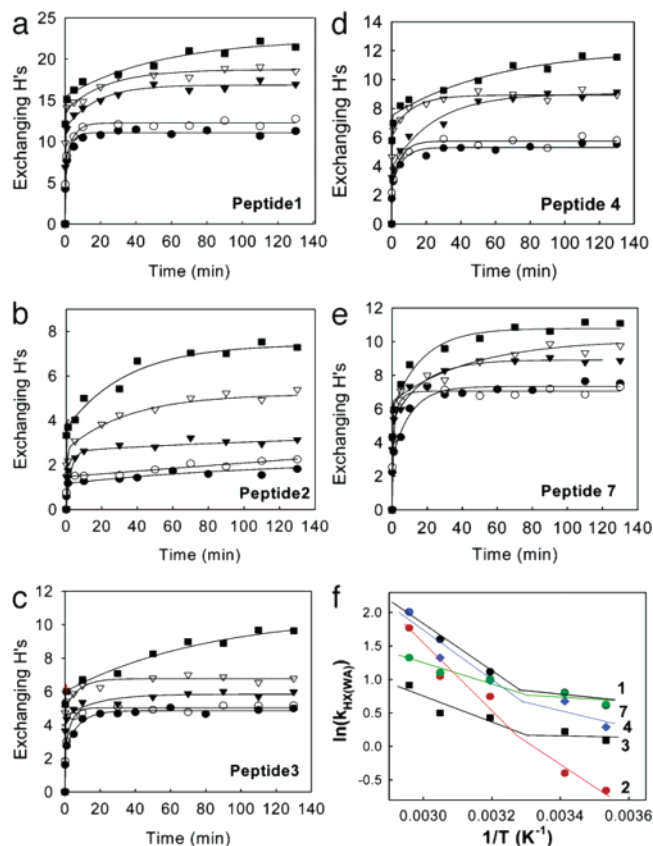
Figure 4. Time courses for hydrogen/deuterium exchange into ht-ADH, which has been digested into 21 peptides. The five peptides of ht-ADH that show a transition in the same temperature range (20−40 °C) as that for the transition in tunneling behavior (30 °C) are shown: 10 °C (closed circles); 20 °C (open circles); 40 °C (closed triangles); 55 °C (open triangles); 65 °C (closed squares). In part f is shown the temperature dependence of the weighted average rate constant for H/D exchange at each temperature for peptides 1−4 and 7. Reproduced with permission from ref 55. Copyright 2004 National Academy of Sciences, U.S.A.

protein motions in achieving the optimal active site configurations for hydride transfer.

2.2.2. Comparison between the ht-ADH and a Psychrophilic Homologue (ps-ADH)

The ps-ADH from the Antarctic strain *Moraxella sp.* TAE 123 is 76% homologous to ht-ADH,[59] yet this protein undergoes denaturation above ca. 35 °C, functioning naturally at ca. 5 °C. In an effort to discern the features that distinguish ps-ADH from ht-ADH, a combination of kinetic and H/D exchange studies were undertaken.

With regard to rates of enzyme turnover, the ps-ADH and ht-ADH display similar k_{cat} values at 20 °C, 4.1 and 8.6 s^{-1}, respectively. Temperature-dependent studies indicate, however, that the $\Delta H^{\ddagger}$ values that control these rates are very different, 21 and 9 kcal/mol, for ht-ADH (below 30 °C) and ps-ADH, respectively.[60] This means that as the temperature is lowered to 5 °C, the activity of the ps-ADH becomes marginally better than that of ht-ADH under conditions of substrate saturation. The K_m for substrate (benzyl alcohol) is quite high for ps-ADH (in relation to ht-ADH), implying that ps-ADH would be a poorer catalyst than ht-ADH at low temperature under conditions of low substrate.[61] However, the substrate-employed (benzyl alcohol) is a non-natural substrate that enables the hydride transfer step to be studied,
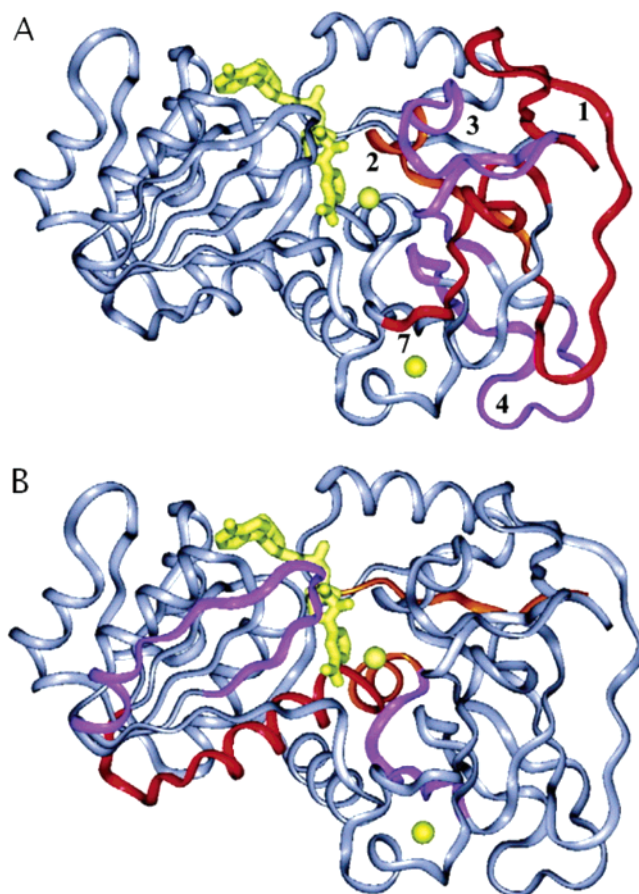

Figure 5. (A) Structural representation of the peptides showing a temperature-dependent transition in H/D exchange behavior between 20 and 40 °C (cf. Figure 4): peptide 1, red; peptide 2, orange; peptide 3, purple; peptide 4, purple; peptide 7, red. (B) Those peptides showing a transition in H/D exchange between 40 and 55 °C (orange, red, and purple). Reproduced with permission from ref 55. Copyright 2004 National Academy of Sciences, U.S.A.

and there is no information on k_{cat}/K_m values for other alcohol substrates.

It seems most likely that the ps-ADH evolved from its higher temperature homologues, and there may not have been much evolutionary pressure to increase its activity above that of ht-ADH in its low-temperature regime (a possible result of sluggish turnover rates for companion enzymes in the psychrophilic cell line). Yet, the ps-ADH has changed its properties in a number of distinguishing ways. First, there is the decrease in its $\Delta H^{\ddagger}$ by 12 kcal/mol, which is coupled to a decrease in $T\Delta S^{\ddagger}$ by 12.5 kcal/mol.[60] This type of compensation between $\Delta H^{\ddagger}$ and $\Delta S^{\ddagger}$ has been seen previously when comparing psychrophilic and thermophilic enzymes,[62] though the studies of ps-ADH and ht-ADH represented the first time that activation parameters on a single chemical step were compared.

One of the most interesting aspects of the comparative study of thermophilic and psychrophilic ADHs has been the finding of the large change in sign for $T\Delta S^{\ddagger}$ for ht-ADH above and below 30 °C and between ht-ADH and ps-ADH below 30 °C. It has been suggested that the $T\Delta S^{\ddagger}$ values may reflect ground-state protein/solvent mobility that is too rigid for ht-ADH below 30 °C and too floppy for ps-ADH and ht-ADH under the conditions of temperature under which they normally function. The implication is that the interior flexibility of proteins has undergone adjustment to accommodate the requirements of their chemical catalysis.

This particular aspect was investigated further by extending the H/D exchange methodology used with ht-ADH to the ps-ADH system. An initial, very surprising finding was that the overall global flexibility for ps-ADH at 4 °C, measured using FT-IR, is less than that seen earlier with either YADH at 25 °C or ht-ADH at 65 °C.[59] Note that YADH and ht-ADH show similar, enhanced global exchange properties when studied at their physiologically relevant temperature.[54] The H/D exchange studies of ps-ADH were then extended to include limited proteolysis of the exchanged protein and mass spectrometric analysis of the resulting, deuterium enriched peptides.[59] Given the different primary sequence for ht-ADH and ps-ADH, somewhat different peptides resulted from limited proteolysis. A total of five homologous peptides and five "bundled" peptides were obtained, representing ∼75% of the polypeptide chain. Among the peptides that could be compared between ht-ADH and ps-ADH, one pair showed similar exchange and four pairs indicated reduced exchange for the ps-ADH in relation to ht-ADH. The remaining five peptides indicated increased deuteration for the ps-ADH.

Although an X-ray structure for ps-ADH is not yet available, its high homology to ht-ADH has permitted a predictive model to be constructed.[59] Mapping of the five peptides with increased H/D exchange onto the tertiary structure for ps-ADH showed that these peptides are in regions of the protein that accommodate substrate and cofactor, consistent with the view that adjustments in *local flexibility* around the active site are necessary to achieve effective hydride transfer rates.[55,63−65] It has been proposed that the relatively low catalytic activity for ps-ADH at 5 °C, a consequence of its highly negative entropy of activation, may, in fact, be a consequence of the presence of too much ground-state flexibility in the enzyme active site.

2.3. Toward an Integrative Model of Tunneling and Dynamics in ADH

2.3.1. Tunnel Correction Models

Invocation of a tunneling correction had been the "first line of defense" in explaining the kinetic aberrations detected in the ADH reaction. According to Bell,[2] H-transfer can be formulated in the context of semiclassical transition state theory by introducing a multiplier term that is isotope-dependent and describes the relative propensity for an isotope to move through rather than over the top of the reaction barrier. As illustrated in Figure 6, barrier penetration is predicted to be greatest for the lightest isotope of hydrogen, leading to isotope effects than can exceed the semiclassical limit ($k_H/k_D \sim 7$ for C−H cleavage) and to isotopic differences in enthalpies of activation and Arrhenius prefactors that lie outside of the semiclassical limit, cf. Table 2. When tunneling occurs in an isotope-dependent manner, the reaction trajectory is different for each isotope of hydrogen, with barrier crossing closer to the classical transition state in the case of the heaviest isotope. It is precisely this behavior that led to the prediction of deviations from Swain−Schaad relationships based solely on zero point energy effect differences among H, D, and T (eqs 5 and 6). In an early study, Rucker et al. attempted to calculate the magnitude of the primary and secondary kinetic isotope effects observed in the ADH reaction by calculating both the semiclassical isotope effects and a tunneling correction in order to match the calculated and observed numbers.[66]
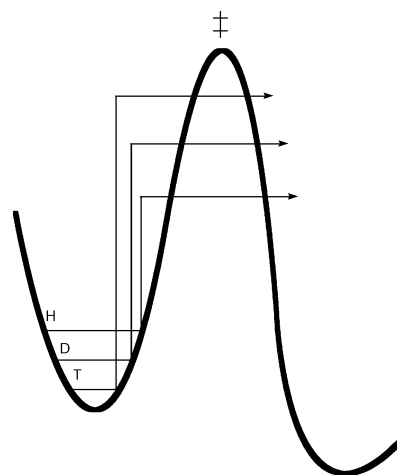

Figure 6. One-dimensional barrier penetration model invoked in the context of a tunneling correction. The lighter isotopes tunnel lower down in the barrier, generating elevated isotope effects, differences in enthalpies of activation that exceed the semiclassical limit, and values for $A_H/A_D \ll 1$.

Their results indicated that it was relatively easy to reproduce the primary H/T and D/T isotope effects as well as the secondary H/T isotope effect. Severe difficulty was, however, encountered when it was attempted to calculate the secondary D/T effect, which was always calculated to be too large in relation to the measured value. Eventually, by coupling a great deal of heavy atom motion into the reaction coordinate (involving atoms from both the cofactor and alcohol substrate), the experimental numbers could be matched. This study, though quite simplistic, pointed out the importance of coupling both heavy atom motions and tunneling into the reaction coordinate.

An important advance that goes beyond the simple Bell correction is the variational transition state theory, which first defines a barrier describing the hydrogen transfer coordinate and then allows each of the isotopes of hydrogen to cross at a certain point below the top of the barrier (corner cutting).[67,68] Initially, such barriers were treated as static entities and ascribed primarily to the C−H stretching coordinate. In recent years, and in recognition of the likely participation of the protein motion in the chemical step, a combined quantum mechanics/molecular mechanics method has been employed in which the protein is divided into two regions: the active site, which is treated quantum mechanically, and the remainder of the protein, which is treated using molecular mechanical force fields. While the QM region is by definition a dynamical one, the MM region was, at first, restricted to a static state. Initial studies of the HLADH reaction using this approach indicated once again that the experimentally aberrant secondary isotope effects could only be rationalized following inclusion of a significant tunneling correction, initially estimated as ca. 60% of the reaction flux.[69]

More recently, the MM region has been allowed to sample different spatial configurations and the impact of this sampling on the hydrogen transfer probability computed. This behavior is referred to as ensemble averaging and takes into account the fact that particular configurations are expected to facilitate the barrier crossing for the transferred hydrogen. These calculations are able not only to reproduce the size of the isotope effects but also to delineate the contribution of various residues within the active site to the H-transfer process.[70] Note that, in these calculations, tunneling is still estimated as a correction to the semiclassical rate by

introducing a κ term that reflects the rate with tunneling divided by the rate in the absence of tunneling. One of the very interesting aspects of these newer multidimensional approaches to tunneling in hydride transfer reactions is that the motion of the environment (protein) is contributing to the potential energy surface in such a way that the barrier begins to resemble those described by Marcus theory for electron transfer (eq 1); that is, the net barrier contains many heavy atom motions that are necessary to achieve the correct configuration for H-transfer/tunneling to occur.[71] In a related study, Cui and Karplus have applied QM/MM calculations to the ADH reaction, concluding that tunneling is playing a relatively small though significant role and that dynamical effects on the barrier are largely the effect of fairly local changes in the positions of active site residues.[72]

With the increasing recognition of a role for protein motions in promoting hydride transfer in ADH, a number of authors have pursued this aspect of the reaction. Bruice pointed out early that the cofactor conformation itself was likely to impact the reaction coordinate, with changes in bond angles within the cofactor bringing the donor and acceptor heavy atoms closer together.[73] In subsequent molecular dynamics calculations, residues were ranked as either correlated (moving together) or anticorrelated (moving in opposite directions), with the anticorrelated motions within the cofactor and substrate binding domains proposed to contribute to the reactive configurations leading to catalysis.[74] Schwartz and co-workers have developed a very interesting algorithm for identifying promoting modes in proteins.[75] Using computer modeling with HLADH, they "scale" various active site residues with regard to the likelihood that their motions will be linked to the hydrogen transfer step.[76] The sequence motif of protein promoting vibrations calculated for HLADH may be conserved among a larger group of ADHs, suggesting a possible conservation of three-dimensional structure that links protein motions to the H-transfer coordinate.

2.3.2. Full Tunneling Models

Although deviations from the Swain–Schaad relationship have been used most frequently as probes of tunneling in the ADH reactions, in other enzyme systems either the size of the isotope effect or its temperature dependence has provided the bulk of the evidence for nonclassical behavior. In this context, the study of ht-ADH is of great value, given the fact that both temperature dependencies of the isotope effects and Swain–Schaad values have been measured between 5 °C and 65 °C. In particular, the transition in enzyme structure and flexibility that occurs at 30 °C changes the properties of both $A_{(light)}/A_{(heavy)}$ and EXP (Table 3).

One particularly notable feature of the data in Table 3 is the weak temperature dependence of the kinetic primary isotope effect above 30 °C. This type of behavior has now been seen in numerous enzyme systems[4,77−82] and is contrary to the expectations of a "tunneling correction model", which predicts a greater temperature dependence for the transfer of the heavier isotope than protium and hence a value for $A_{(light)}/A_{(heavy)} \ll 1$ (Figure 6). The observed invariance of the kinetic isotope effect with temperature is most generally interpreted in the context of full tunneling models, where the barrier to reaction is attributed to the heavy atom motions that affect the probability of wave function overlap. A simple model that provides a useful physical picture has been presented in the context of the enzyme soybean lipoxygenase

and is referred to as an "environmentally coupled tunneling model".[4] Though the heavy atom motions are expected to participate in a variety of ways, it is useful to divide these motions into two basic terms: those that affect the relative energy levels of reactant and product and those that affect the distance between the H-donor and acceptor (Figure 7). The former can be treated via a Marcus-type term in which the dominant parameters are λ, which describes the inner and outer sphere reorganization, and $\Delta G°$, which is the reaction driving force (cf. Figure 1). In the case of an impact of distance sampling on tunneling, this can be described via a Frank−Condon term for wave function overlap that is integrated over a range of donor acceptor distances.[4,52]

One of the benefits of this type of description of H-transfer is that it can explain nearly temperature-independent isotope effects—attributed to little or no sampling of the distance between the reacting atoms—and a dominance of the barrier crossing between ground-state vibrational modes of reactant and product. As a corollary, when distance sampling begins to become important, the temperature dependence of the isotope effect is predicted to increase, reflecting the requirement of a shorter distance for deuterium or tritium to undergo transfer (a consequence of their shorter inherent wavelengths relative to protium).

Of significance to this model, examples of enzymes have emerged that show a change in behavior from an approximately temperature-independent isotope effect for WT-enzyme to a more temperature-dependent isotope effect when the protein has been perturbed via site-specific mutagenesis.[4,52,83] This pattern is also seen with ht-ADH, though in this case the perturbant is temperature. As summarized in Table 3, the magnitude of $A_{(light)}/A_{(heavy)}$ has become inverse below 30 °C. The most likely explanation for this trend in $A_{(light)}/A_{(heavy)}$ is the inability of the more rigid protein below 30 °C to generate a precise alignment (preorganization) of the donor and acceptor atoms in the Michaelis complex; this introduces a requirement for distance sampling and, hence, a temperature dependence to the measured isotope effect. By contrast, at the elevated temperatures, ht-ADH is postulated to possess enough thermal flexibility to achieve optimal alignment (preorganization) between the H-donor and acceptor. Under these conditions, distance sampling will be minimized and the isotope effect behaves in an approximately temperature-independent manner.

How then do the observed values for EXP fit into this picture of tunneling? One fascinating aspect of the ht-ADH data is the finding that the value of EXP is most inflated when the temperature dependence of the isotope effect is small. Within a "tunneling correction model," it would be the greater barrier penetration for H than D that inflates the magnitude of EXP. *But this is precisely the condition that is expected to produce a value for $A_{(light)}/A_{(heavy)}$ that is less than unity—in contrast with the experimental observations.* A more satisfactory interpretation of the Swain−Schaad deviations was, therefore, sought in the context of a "full tunneling model." According to the picture that is evolving, it is crowding within the enzyme active site that produces the anomalous EXP observations.[3] When the protein active site is optimized, as is postulated for the WT-ht-ADH at the elevated temperature, the distance between donor and acceptor is already quite short for H-transfer. In the case of D, the need for a somewhat shorter distance may reduce the capacity of the reacting bonds to undergo the rehybridization that is expected to accompany the hydrogen transfer (analo-
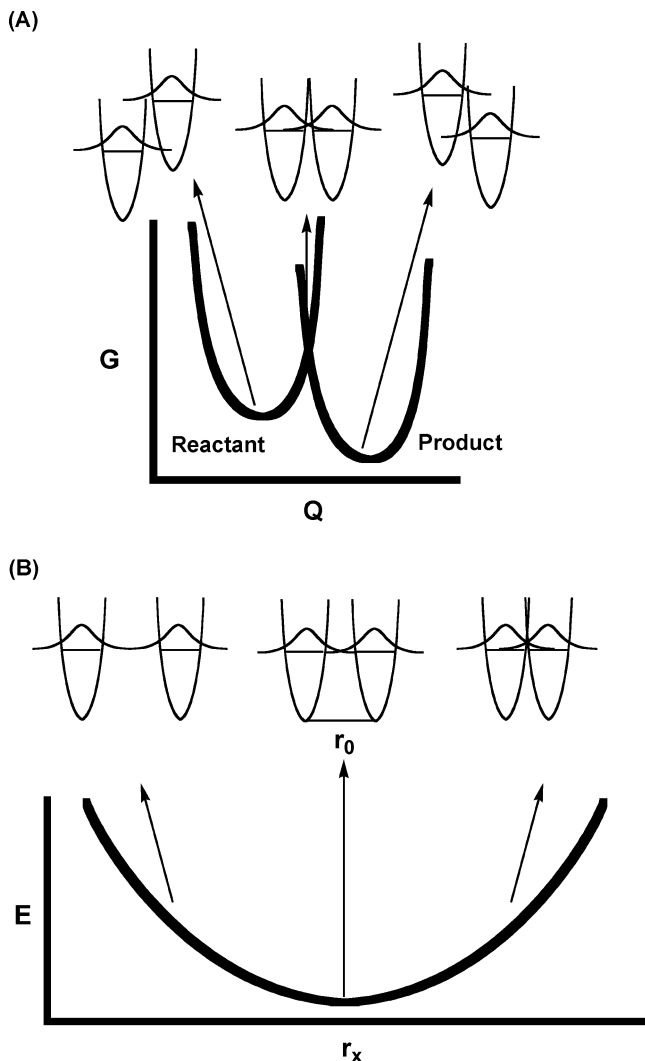
(A)

(B)

Figure 7. An expanded Marcus model applied to hydrogen transfer. The nuclear coordinates are represented by Q, the donor acceptor (gating) coordinate is represented by r_x, and r_o is the initial equilibrium distance. Panel A is analogous to classical Marcus theory in that heavy nuclear reorganization (the free energy for this process is represented by the heavy lines as a function of progress along the coordinate Q) is required before significant tunneling can take place. The main difference is that hydrogen (and not electron) wave function overlap determines the tunneling probability. At the transition state, corresponding to the intersection of the heavy lines, the hydrogenic potential surfaces are isoenergetic with respect to hydrogen transfer, so that transitions (tunneling) can take place between them in accord with the Franck−Condon principle. Panel B illustrates how, once this configuration is reached, hydrogen wave function overlap can be enhanced by bringing the donor and acceptor closer together. Assuming that the donor−acceptor distance is governed by a harmonic potential, the ability of thermal fluctuations to compress the oscillator by an amount Δr below its equilibrium configuration r_o will depend on the force constant describing the curvature in the potential well. The distance r_x is where the balance between interatomic repulsive forces and efficient wave function overlap is optimal. It is anticipated that, for many enzyme active sites, the well will be relatively stiff, so that the donor−acceptor distance remains near r_o, and gating effects are minimized. Reproduced with permission from ref 52. Copyright 2005 Elsevier.

gous to the inner sphere reorganization described in the Marcus theory of electron tunneling).[19] This will suppress the magnitude of the experimental secondary D/T isotope effect in relation to H/T, which presumably retains sufficient space for bond rehybridization to accompany the protium

wave function overlap from donor to acceptor atoms. This active site configuration is predicted to produce EXP > 3.26 and A_H/A_D > 1 (Figure 8A).

The above view can be extended to the low temperature regime for ht-ADH, where H/D exchange experiments implicate a more rigid protein structure and less efficient preorganization in the vicinity of the cofactor and substrate binding sites. Under this condition, the tunneling of both protium and deuterium may be expected to take place from a more extended distance. This phenomenon produces two effects: the first is a relatively poor wave function overlap in the case of D-tunneling, introducing the need for increased distance sampling (leading to more temperature-dependent isotope effects). The second is a reduction in crowding for both H- and D-transfer (permitting significant inner sphere reorganization for D-transfer, as well as H-transfer, and an EXP that appears more semiclassical in its behavior). Both of these behaviors are illustrated in Figure 8B.

The model invoked to describe the behavior observed with ht-ADH also offers a reconciliation of the unexpected trends for the secondary isotope effects summarized in Table 1 for YADH and HLADH. As noted earlier, altering either the substrate (with YADH) or the protein (for HLADH) leads to secondary H/T isotope effects that are essentially unchanged whereas the D/T undergoes a systematic increase in value. Of particular relevance to the new "full tunneling model" that is being advanced for the ht-ADH,[3] the magnitude of D/T is seen to increase in a regular fashion for the active site mutants of HLADH that expand the active site geometry. [Note the X-ray structure reported for V203A,
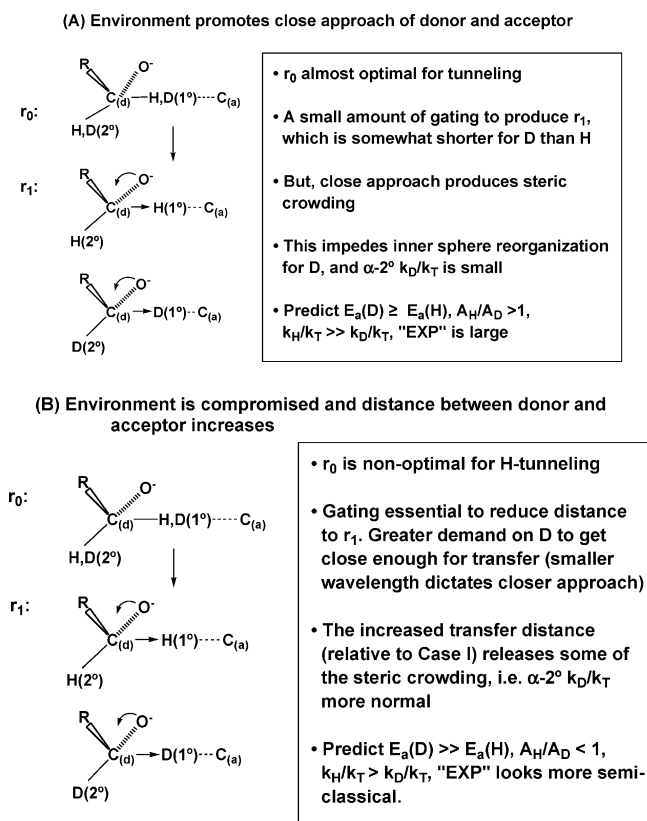

Figure 8. Two scenarios for enzyme active sites can be envisaged. According to (A) the protein dynamics and active site environment promote close approach between the H-donor and acceptor, leading to A_H/A_D > 1 and EXP > 3.26. For a "compromised" active site, a greater initial distance between the donor and acceptor atoms generates A_H/A_D < 1 and EXP ≅ 3.26.

(A) Pre-organization
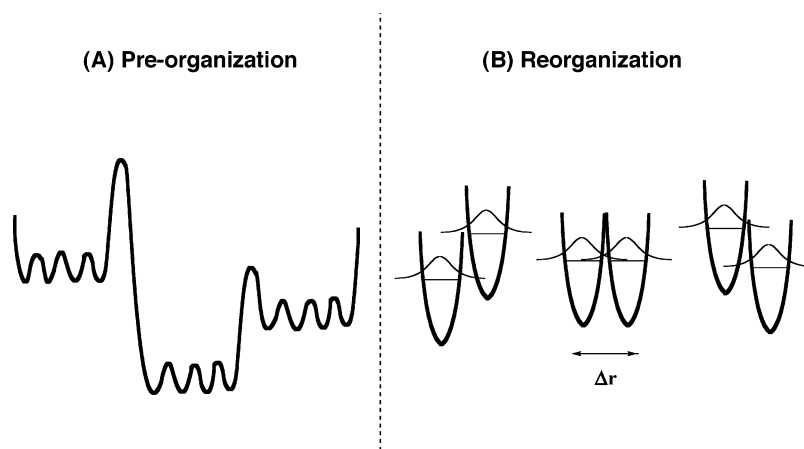
(B) Reorganization

Δr

Figure 9. Distinction between the types of motion expected to be critical to enzymatic H-transfer. On the left (A) is the "preorganization" term that involves a rapid sampling (ns−ms) of multiple configurations, preventing the active site from becoming trapped in a local minimum with a less optimal arrangement of bound substrates. On the right (B) is the subsequent "reorganization" of bound substrates. This is expected to involve even more rapid sampling (ps−ns) of states that differ with regard to the relative energy levels of reactant and product and the distances between reactants. The isotope dependence of the isotope effect comes primarily from the distance sampling component of the reorganization term. When distance sampling has been minimized, as a result of effective preorganization events, the isotope effect can appear temperature-independent.

which showed an increase of ca. 0.8 Å between the C-1 of an analogue of the alcohol substrate and C-4 of the cofactor acceptor[35] (Figure 2).]

Though the ideas developed above and in ref 35 will require further experimental testing for verification, they offer a new and exciting perspective from which to view the hydride transfer reactions occurring in the ADH reaction. To recapitulate, the best model that can currently be advanced invokes a full tunneling picture, with the efficiency of tunneling dependent on the capacity of the protein to optimize the distance between the donor and acceptor atoms. It is precisely this optimization that is proposed to lead to the observed anomalies in experimental parameters that include largely temperature-independent isotope effects and inflated exponents for the Swain−Schaad relationship (eq 5).

The role for protein dynamics in facilitating H-transfer needs to be revisited in the context of these new views. Our perspective is that protein flexibility, modulated by residues that are both local to and distal from the active site, is an essential feature in creating the optimal geometry between the H-donor and acceptor. We refer to this contribution of protein motion as the "coarse tuning" or "preorganization" (Figure 9A). Once configurational sampling of the protein landscape has been achieved, additional heavy atom motions participate in the H-transfer reaction, termed the "fine-tuning" or reorganization (Figure 9B). This includes both λ (the environmental reorganization term, which, though reduced in relation to its value for a comparable reaction in solution, is still expected to represent the major portion of the activation barrier controlling the H-transfer processes) and the modes that alter the distance, r, between the H-donor and acceptor (affecting the temperature dependence of the isotope effect). The impacts of λ and r have been illustrated in Figure 7. We note that following the preorganization of the protein the force constants for motion within the Michaelis complex may become fairly stiff (in relation to kT), reducing the extent to which motions that control distance sampling undergo excitation. In the event that a protein is unable to accomplish this type of optimization (or has been compromised via mutagenesis, introduction of a nonoptimal substrate, or a change in temperature in the case

of a thermophilic protein), the degree of distance sampling may be expected to increase.

3. Dihydrofolate Reductases

As with alcohol dehydrogenase, dihydrofolate reductase (DHFR) is a ubiquitous, well-studied enzyme that has served as a paradigm for investigating enzyme catalysis. DHFR catalyzes the stereospecific transfer (eq 10) of the *pro-R*

$$(10)$$
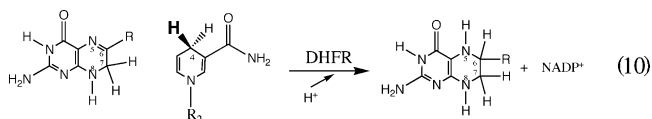
hydrogen from the 4 position of NADPH to dihydrofolate (DHF) to yield tetrahydrofolate (THF).[84] The *pro-R* hydrogen is indicated in boldface type, R represents the *p*-aminobenzoylglutamate moiety of THF, and R_2 represents the adenosyl ribose moiety of NADPH.

Studies of *E. coli* DHFR (ec-DHFR) have revealed that there is a preferred kinetic pathway for substrate binding (Figure 10). This diagram demonstrates the complexity that can arise in a 2-substrate/2-product enzyme-catalyzed reaction. The "preferred" pathway is the one along which the rate constants are fastest, but mutants can, in principle, lead to a different pathway by making one step much slower. The rate of hydride transfer is fastest at low pH with a rate constant of 950 s^{-1} when all of the enzyme is in its protonated form.[84] By going off the pH optimum (to pH 9) or using stopped flow kinetics, it has been possible to show that the size of the isotope effect on k_{cat} is ca. 3, very close to the value seen in the hydride transfer catalyzed by the alcohol dehydrogenases. These two examples illustrate the commonly smaller primary deuterium isotope effects seen for hydride transfer reactions, in relation to enzyme-catalyzed free radical reactions (cf. ref 4).

3.1. Evidence of Motion

In the case of alcohol dehydrogenase, the role of tunneling in catalysis was the focus of early investigations, with
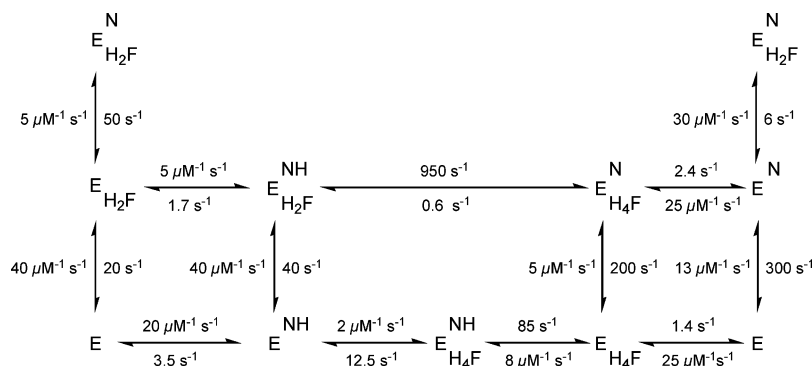
Figure 10. Kinetic mechanism of DHFR at 25 °C, where rate constants pertain to the protonated enzyme. The kinetic species represented by the abbreviations are as follows: N, NADP$^+$; NH, NADPH; H$_2$F, dihydrofolate (referred to as DHF in the text); H$_4$F, tetrahydrofolate (referred to as THF in the text). Reproduced with permission from ref 98. Copyright 2006 Annual Reviews.
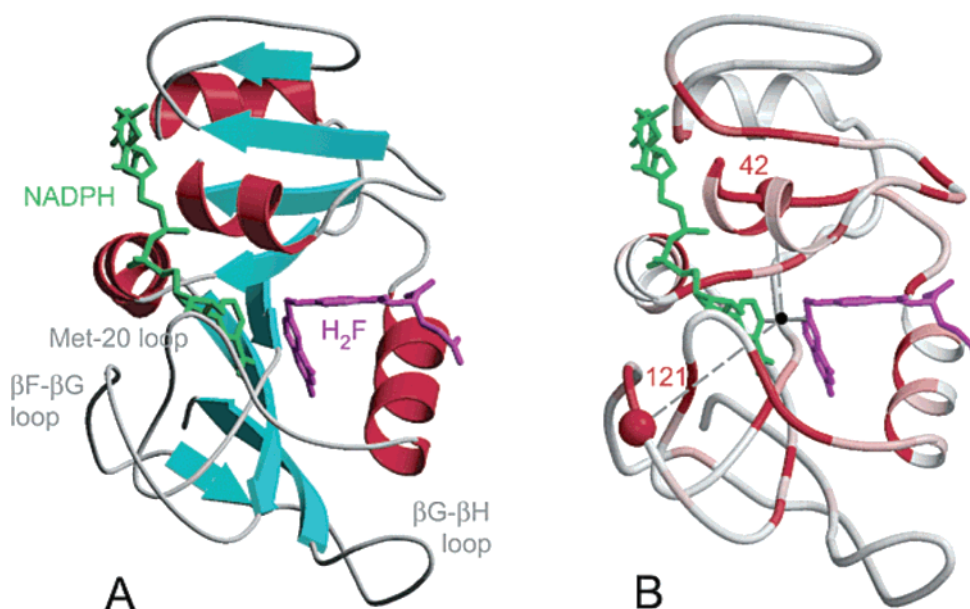

Figure 11. X-ray structure of *E. coli* dihydrofolate reductase modeled to be complexed with NADPH and DHF(H$_2$F). (A) indicates mobile loops in gray, and (B) shows the location of conserved residues (red) and specifically G121 and M42 (red spheres). The black sphere indicates the position of hydride in the active site. Reproduced with permission from ref 125. Copyright 2002 American Chemical Society.

dynamics being invoked primarily during the last five years. By contrast, early studies of DHFR centered on the role of dynamics, and only recently has tunneling been embraced as an important contributor to catalysis. In both enzymes, however, it was early studies based on classical kinetics that inspired the explosion of research that followed.

3.1.1. Substrate-Induced Conformational Changes

Early studies of NADPH binding to DHFR from *L. casei*[85] had indicated that the enzyme existed in two interconverting forms, only one of which bound cofactor: more recent detailed kinetic analysis of the enzyme has provided further evidence of multiple conformations that depend on the liganded state. The five intermediates shown in Figure 10 for ec-DHFR could be resolved kinetically using stopped flow and fluorescence techniques.[84] In addition to their utility in determining the kinetic mechanism, the spectroscopic changes provided evidence for the contribution of conformational changes prior to the hydride transfer step.

3.1.2. Crystal Structures of Intermediates (with Analogues)

Using substrate and transition state analogues, Kraut and co-workers were able to create a "movie" describing the

conformational changes that take place along the reaction pathway.[86] The enzyme was incubated with NADP$^+$, NADPH, ATP−ribose, folate (analogue of DHF), methotrexate (analogue of the transition state), and 5,10-dideazatetrahydrofolate (analogue of THF). Structures were determined for five complexes, corresponding to the kinetically observable intermediates, and for one complex with methotrexate, attributed to the transition state. The structure for *E. coli* DHFR modeled to be complexed with NADPH and DHF is shown in Figure 11.

Among the most dramatic changes were those seen in the M20 loop, which had earlier shown evidence of mobility in X-ray structures and NMR experiments. This loop closes over the active site in the complexes corresponding to the enzyme binary and ternary complexes formed with NADPH, DHF, and methotrexate. In the product complexes that bind NADP$^+$, THF, and finally NADPH, the loop moves to an "occluded" conformation in which it protrudes into the active site. These two conformers for the M20 loop have been implicated in the catalytic cycle. There is an additional conformation that may allow substrates and products to diffuse into and out of the active site. Though the above picture was developed through the use of substrate and transition state analogues, NMR, kinetic, and single molecule

experiments (see below) have supported many of the X-ray-based structure conclusions.

3.1.3. NMR Studies of DHFR

NMR can serve as a powerful experimental probe of protein motion on the time and distance scales predicted to be important for catalysis. Unlike single molecule (see below) and many other probes of dynamics that measure a single fluctuating parameter, NMR can monitor the entire protein at once. Although recent advances and their application to DHFR have been reviewed rather extensively,[87] a few key experiments are briefly summarized as they relate to dynamics on different time scales that may be linked to the hydride transfer step.

One method that has been used increasingly is the evaluation of order parameters. These contain information about the time scale of internal protein motion and are calculated from the nuclear spin relaxation properties. Motions were detected in DHFR in the flexible loop regions on the nanosecond to picosecond time scale, and these were altered depending on the liganded state of the enzyme, corroborating growing evidence that the dynamical properties of the protein change over the course of the catalytic cycle.[88]

Motion on the millisecond time scale has been observed by relaxation dispersion experiments, which take advantage of differences in chemical shifts between conformers. This method has been applied to ^{15}N-substituted ec-DHFR to probe backbone fluctuations in the active site. In the complex of NADPH and the substrate analogue folate, most residues appeared to be exchanging between two chemical shifts on the millisecond time scale, suggesting transitions between two conformers.[89] One of these was sparsely populated (~5%), with chemical shifts consistent with the occluded conformer of DHFR in which the M20 loop protrudes into the active site. Based on the exchange kinetics, the conformational transition from closed to occluded was concluded to occur more slowly than hydride transfer and to provide a means of confinement of NADPH in close proximity to the substrate.

As a complement to the investigation of backbone dynamics, NMR studies were also carried out to determine the dynamical properties of side chain methyl groups.[90] These were measured by two complementary means, involving the determination of order parameters and side chain rotamer populations for methyl groups. Order parameters determined for side chains in DHFR complexed with folate were compared to averages measured in other proteins. As might be expected, some residues in the mobile FG loop were more disordered, though residues in and near the substrate-binding pocket (including M42) had properties consistent with relatively restricted motions. This restriction increased in the ternary complex with NADPH, with the largest increases appearing in a network of hydrophobic residues in the nicotinamide-ribose binding pocket and the active site. Flexibility is lost upon ligand binding, particularly around the active site, as the protein attains the configuration optimal for catalysis.

Side chain rotamer populations were determined in the same binary and ternary complexes for which order parameters had been obtained.[90] In both complexes, most side chains favored the rotamers observed in the X-ray structure. In some cases, where X-ray structures indicated disorder for a particular side chain, rotamer averaging was observed in the NMR experiment. Most interesting were residues, mostly

in and near the active site, that showed rotamer averaging in NMR but had a well-defined orientation in the crystal structure. Of particular interest are the hydrophobic active site residues Ile14 and Ile94, which in the crystal structure are in van der Waals contact with substrate and cofactor, and occupy only one rotamer (Figure 12). The NMR data
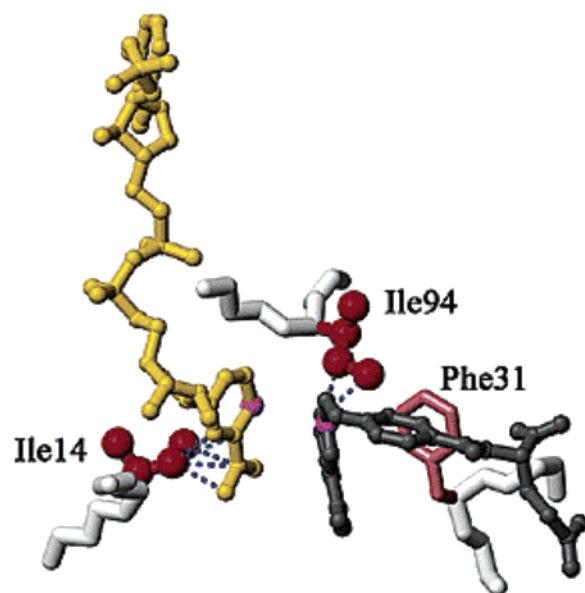

Figure 12. Hydrophobic residues at the active site of ec-DHFR that are proposed to control the relative position of NAD^{+} and substrate. Side chains of residues 14 and 94 are shown in red spheres, NAD in yellow, and folate in black. Reproduced with permission from ref 90. Copyright 2004 American Chemical Society.

indicate that this rotamer of Ile14 dominates when the ternary complex is in solution, but another rotamer is also significantly populated. If the side chain were to take on the latter configuration in the X-ray structure, it would clash with the nicotinamide ring in such a way as to force it toward the pterin ring of the substrate. The situation is similar for Ile94, which clashes with both the pterin ring and Phe31 in the rotamer that is populated in solution, but not in the X-ray structure. Taken together, these motions suggest a means by which the enzyme could modulate the hydride donor acceptor distance. Resonance broadening observed for Ile 14 indicates that transitions between rotamers may take place on the millisecond to microsecond time scale, consistent with motion predicted in simulations.[91]

3.2. Impact of Mutations on Catalysis and Protein Mobility

Both NMR and X-ray data provide convincing evidence for mobility in the loop regions in DHFR. Given that changes in the M20 loop structure are a major distinguishing factor among the DHFR complexes, a change in this region of protein can be comfortably concluded to occur during the overall chemical transformations of the catalytic cycle. It is a natural extension to consider whether the flexibility of the M20 (and other loops) plays a direct role in the chemical, hydride transfer step.

The first kinetic evidence of such a dynamical role for residues distal to the active site came when residues 16−19 of the M20 loop were replaced with a single glycine residue in *E. coli* DHFR.[90] Crystallographic evidence suggested that the mutation would not significantly alter either the global

structure of the enzyme or that of the active site, but the effect on catalysis was dramatic. The value of the rate constant for C−H cleavage decreased from 950 to 1.7 s^{-1}. Two-dimensional NMR experiments carried out on both the wild-type and mutant proteins indicated an exchange process consistent with a relatively slow dynamical process (millisecond time scale) in the wild type. The process was absent, however, in the protein containing the M20 loop deletion, thus demonstrating a relationship between protein dynamics and the efficiency of hydride transfer.

NMR was used again[88] to identify other regions of DHFR that are most mobile in solution. Two-dimensional H−N relaxation methods, as a probe of dynamics and fluctuations on the nanosecond time scale, pointed to a possible role of the β-F/β-G loop (cf. Figure 11). Given the conformational flexibility conferred by the lack of a side chain at glycine 121 within this loop, replacement by valine was carried out, leading to a decrease in the rate of hydride transfer by nearly 500-fold.

An extensive sequence alignment of EcDHFR homologues revealed that a number of positions distal to the active site, including G121, are conserved.[92] Interestingly, many of these residues tend to fall within loops that had been shown to be flexible using crystallography and NMR. One strongly conserved residue is M42, located in a β strand, 15 Å from the active site, and on the side of the protein opposite from G121 (Figure 11). A series of single site mutants at position 42 were all found to decrease the hydride transfer rate significantly, implicating M42 as well as G121 in the chemical step.

Given the placement of G121 and M42 on opposite sides of the DHFR active site, a logical next step was to examine the impact of double mutations on catalysis. In proceeding from single to double mutations within a protein, it has often been predicted that the impact of noninteracting residues will be additive.[93] Though this can be a dangerous assumption to make for residues within an active site or in close proximity within a protein,[94] the assumption may become a reasonable one when the residues undergoing change are located quite far away in space. In the case of DHFR, the double mutant, G121A and M42F, showed a rate reduced from that predicted from the sum of the single mutation data, leading to the proposal of a coupled network of residues that traverses the active site. It has been noted that nonadditivity can be due to an artifactual change in rate-determining step-(s), though this seems not to be the case in DHFR. It would appear that such an apparent nonadditivity may also arise from an equilibration between active and inactive forms of enzyme that effectively decreases the concentration of active catalyst. As will be discussed below, computational approaches support the view of a coupled network of motions that is linked to the hydride transfer step in DHFR.[91,95]

3.3. Single Molecule Experiments

Single molecule experiments have been carried out in order to investigate directly the structural changes associated with substrate/cofactor-binding and possibly catalysis. In light of the proposed significant role for the M20 loop in these phenomena, Hammes and co-workers appended the fluorescent molecule Alexa 488 to position 18 in DHFR from *E. coli* via coupling to an engineered cysteine.[96] The results indicate a number of time-dependent changes, some of which correlate with rate constants determined previously by transient state kinetics, and some of which are unique to these single molecule experiments.

A major advantage to single molecule experiments is that phenomena obscured in the ensemble average, such as multiple protein conformers and both static and dynamic disorder in rate constants, can be resolved. Single molecule experiments provide an experimental test for the detailed predictions made by simulations, because other sensitive probes of dynamics (NMR, X-ray, bulk fluorescence, Mossbauer, etc.) are averaged over many molecules and are not always time-resolved. This makes it difficult to tell the order in which two dynamical events occur, whether they are correlated, and whether they are happening on the same molecule.

In one investigation, binding of methotrexate to DHFR and the dynamics of DHFR bound to this potent inhibitor were studied.[96] Binding was monitored in the ensemble via fluorescence quenching of the liganded state, which was (more or less) equally manifest in both the internal (Trp) and Alexa 488 fluorescence. The dye was employed in single molecule experiments because of the intensity of its fluorescence and because its optical properties were more compatible with the available equipment.

A dissociation constant of 9 nM calculated from the ensemble experiments could be qualitatively verified in the single molecule experiments. The behavior of the subset of enzyme molecules bound to methotrexate offered information unavailable in ensemble measurements, namely that the extent of fluorescence quenching is actually a fluctuating quantity. The observed "blinking" of the fluorescence took place on a time scale faster than methotrexate dissociation. This experiment has served as a valuable proof of principle and provided evidence for a role for dynamics within a complex of DHFR and a tightly bound inhibitor.

In experiments with substrates, NADPH, and DHF, similar blinking was observed on DHF binding, and the kinetics were attributed to conformational changes in the E-DHF complex.[97] The kinetics of NADPH binding suggested that the cofactor binds to a different conformation than does the substrate. All measurements were consistent with stopped flow measurements, and the hydride transfer could be followed "directly" because of a change in Alexa 488 fluorescence during the chemical reaction.

For these experiments, fluorescence lifetimes could be measured for enzyme with substrates at equilibrium; only in the presence of substrates were fluctuations on a millisecond time scale observed, and the data allowed the discernment of at least two states. One troubling feature of this aspect of the experiments was that a kinetic isotope effect (seen in the ensemble) could only be observed in the single molecule experiments for the forward reaction. This was attributed to additional complexity in the fluorescence lifetimes that could not be extracted from the data given the experimental signal-to-noise ratio. It is likely that there are multiple exponential processes corresponding to additional steps. Further, it is difficult to differentiate a conformational change that drives the chemical step from one that is a non-rate-limiting accommodation of protein structure to changes in the bound substrates.

3.4. Simulations

Hybrid quantum mechanical/classical molecular dynamics (QM/MD) simulations have increasingly provided insight into the nature of conformational sampling in DHFR and have been reviewed elsewhere.[98] A picture consistent with experimental observations emerges, wherein the mobile loops

implicated in conformational sampling participate in a coupled network of equilibrium motions that, when frozen out, increase the barrier to hydride transfer.

In the wild-type system, the equilibrium average of the donor−acceptor distance was found to decrease significantly at the transition state, along with puckering of the DHF ring. A decrease in the equilibrium distance between Phe31 and DHF could be correlated with these changes, suggesting that motion of this hydrophobic residue is important for catalysis.[91] A common theme to many of the enzymes that transfer hydrogen and are thought to involve tunneling is the importance of conserved active site hydrophobic residues for dynamics and catalysis.

A more recent analysis has explored the correlation between motions in different parts of the protein along the reaction coordinate.[95] It was shown that among motions that take place in concert along the reaction coordinate, some are correlated (moving in the same direction) while others were anticorrelated (moving in the opposite direction); as anticipated, many motions between atoms far from the active site are involved. When calculations were carried out on mutant enzymes, some of the motions were disrupted, and the distances between specific atoms as a function of the reaction coordinate had changed (and presumably were no longer optimal). These works have explored ec-DHFR in the context of the mutants that showed nonadditive effects on the rate of catalysis.[91,95] Differences between the double and triple mutants support the view that effects of the mutants are not statistically independent.

Simulations such as these begin to approach a detailed description of some of the motions that are important for catalysis. However, the described changes in the equilibrium positions of residues, including the hydride donor and acceptor, are best ascribed to relatively slow, preorganizational effects that are distinct from the reorganization and distance sampling (or gating) terms implicit in a modified Marcus model of hydrogen transfer (Figure 7). The demonstration of hydrogen tunneling in the DHFR reaction and its dependence on enzyme source and structure (see below) begins to close the circle, linking protein dynamics to the detailed properties of the hydride transfer step. Of particular note is the temperature-independent kinetic isotope effect for wild-type DHFR[77] that is converted to a temperature-dependent effect upon mutation at position 42[83] (see below). These argue, as with the ht-ADH above 30 °C, for a preorganization that is linked to increased rigidity within the active site of the wild-type enzyme.

3.5. Comparative Properties of Tunneling among Homologous DHFRs.

Based on the behavior of the alcohol dehydrogenases (section 2), it can be anticipated that the tunneling and dynamical properties of DHFR may be sensitive to the environmental niche under which the protein functions. It is therefore of interest to examine whether extremophilic variants homologous to ec-DHFR have adapted their structures to modulate dynamics in a way that can be correlated with catalysis. As discussed below, comparison of the temperature dependences of the kinetic isotope effects for homologous DHFRs reinforces the lessons learned from ADH.

3.5.1. Evidence of Tunneling in ec-DHFR

As outlined in section 2, the temperature dependence of kinetic isotope effects can serve as an informative probe of the nature of the chemical step. An important caveat is that the hydrogen transfer step must be fully rate-determining when such an analysis is undertaken. Given the inherent complexity of DHFR and the need for high precision data, Kohen and co-workers employed experimentally−determined competitive isotope effects to calculate intrinsic kinetic isotope effects as a function of temperature.[77] Their study, analogous to an earlier one on the enzyme peptidylglycine α-hydroxylating monooxygenase,[78] uses the Swain−Schaad relationship to convert experimental isotope effects into intrinsic values as originally introduced by Northrop.[99] It should be noted that the method of Northrop could only be employed when deviations of the Swain−Schaad exponent arise from kinetic complexity and not from tunneling itself. While there is ample evidence for significantly deviant Swain−Schaad behavior describing secondary isotope effects in the alcohol dehydrogenase reaction as a consequence of tunneling, there are no documented examples of such extreme behavior for primary isotope effects with either ADH or other enzyme systems. As noted in the study of peptidylglycine α-hydroxylating monooxygenase, even if the Swain−Schaad relationship were altered somewhat due to tunneling, its property would not be expected to change within the limited experimental temperature range of the enzyme studies,[78] validating the approach taken in both the earlier[78] and DHFR analyses.[77]

Focusing on the computed primary intrinsic isotope effects with wild-type ec-DHFR, two interesting observations were made.[77] Most strikingly, the intrinsic kinetic isotope effects were found to be temperature-independent, within the error of the experiments carried out. In addition, the Arrhenius energy of activation, E_a, was nonzero. DHFR thus joins the growing list of enzymes shown to display this unusual behavior for hydrogen transfer, most often rationalized in the context of a full tunneling Marcus-like model. As shown in Figure 7, E_a arises from the environmental reorganization that must occur before tunneling can proceed. A temperature-independent isotope effect implicates a highly preorganized active site with little need for distance sampling. A secondary observation in this work is the presence of some kinetic complexity across the range of temperatures at which kinetic isotope effects were measured; this may have ramifications for the interpretation of previously reported data.

In separate studies, Kohen and co-workers carried out a similar analysis on the M42W variant of ec-DHFR, observing an increasingly familiar trend in which a perturbation of the enzyme introduces a temperature dependence to kinetic isotope effects.[83] Additionally, the overall value of the primary kinetic isotope effect was seen to be somewhat larger. An explanation analogous to that described for ht-ADH (see section 2 above) and soybean lipoxygenase mutants[4] can be made: Mutations are proposed to perturb the geometry of the enzyme away from its optimum state, impairing preorganization steps (Figure 8A) and increasing the distance between the hydrogen donor and acceptor. This can increase both the size of the isotope effect and the need for a distance sampling mode, to improve the efficiency of the hydrogen wave function overlap. The gating mode will show both temperature and isotope dependence and, thus, can account for the increased temperature dependence of the isotope effect. Of particular interest in DHFR is the creation of a mutation at a long distance from the position of hydride transfer. Whereas previous studies on LADH and SLO focused on more proximal active site hydrophobic residues,
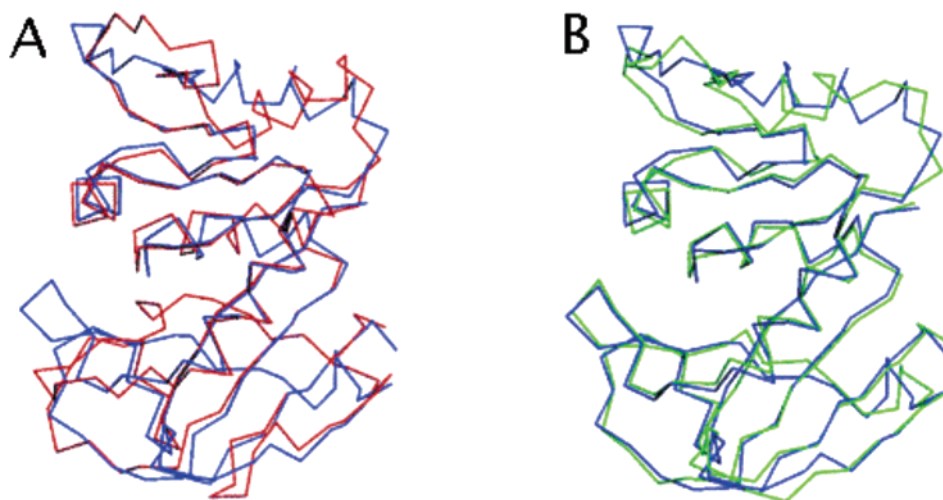
Figure 13. Comparison of X-ray structures of homologous DHFRs. (A) Cα overlay for Bs-DHFR (blue) and tm-DHFR (red) and (B) overlay for bs-DHFR (blue) and ec-DHFR (green). Reproduced with permission from ref 100. Copyright 2005 American Chemical Society

M42W represents a perturbation that lies 15 Å from the active site. Coupled with the wealth of experimental and computational investigations implicating long-range dynamics in DHFR, these data point toward a direct link between the motions at position 42 and the hydride transfer step.

3.5.2. Studies of Hydrogen Transfer in DHFR from a Moderate Thermophile, B. Stearothermophilus (bs-DHFR), and the Hyperthermophile T. Maritima (tm-DHFR)

An X-ray structure has recently been solved for the apo-form of the monomeric DHFR from *B.* stearothermophilus (bs-DHFR), a moderately thermophilic organism that grows optimally around 65 °C.[100] The structure is largely super-imposable with those from ec-DHFR (38% identity, 58% similarity) and a monomer of tm-DHFR (23% identity, 56% similarity), a hyperthermophilic protein that, in contrast to ec- and bs-DHFR, is a functional dimer (Figure 13).

Most of the divergence in sequence for bs-DHFR is in the loop regions. Like other DHFR structures, the M20 loop shows relatively high temperature factors suggesting significant mobility. The betaF/betaG loop, which contains G121 (and has been shown to be important for hydride transfer in ec-DHFR, see above), is flanked by two proline residues in bs-DHFR; this may reflect the need for an attenuation of motion that might disrupt catalysis at the higher functional temperatures. The idea that dynamical features in homologous enzymes are similar at their physiologically relevant temperatures has been supported by NMR experiments.[101]

Kinetic studies carried out on DHFR from *B. stearothermophilus* show, as with other DHFRs,[84] that chemistry is most rate-limiting at high pH, where the observed primary hydrogen isotope effect on k_{cat} becomes equivalent to the value on k_{cat}/K_m(DHF). Transient state kinetics using C-4 protio- and deuterio-labeled NADPH have provided the temperature dependence of the isotope effect, which indicates a value for $A_H/A_D = 0.57$ compared to $A_H/A_D = 4.0$ for the ec-DHFR.

Both steady state and pre-steady-state kinetics have also been conducted with the tm-DHFR, which shows a break in behavior that is somewhat analogous to that seen with ht-ADH.[102] Specifically, there is a weakly temperature-dependent isotope effect for tm-DHFR at the elevated, physiologically relevant temperature, $A_H/A_D \sim 1$, with the isotope effect becoming much more temperature-dependent below 25 °C, $A_H/A_D = 0.002$. In contrast to the different patterns for the temperature dependence of the isotope effect depending on the source of DHFRs, the size of the isotope effect is almost invariant. The rates of reaction for the three DHFRs, however, do show a trend such that k_{cat} (measured at the physiologically relevant temperature of each enzyme) decreases while E_a increases in proceeding from ec-DHFR to bs-DHFR and tm-DHFR (Table 4).

Table 4. Comparison of Kinetic Parameters for Three Homologous DHFRs

enzyme	k_{cat}, s^{-1}, pH 9[d]	E_a, kcal/mol	A_H/A_D	k_H/k_D[e]
EcDHFR[a]	16 (25 °C)	3.0	4.0 (1.5)	3.4
BsDHFR[b]	4.8 (60 °C)	5.5	0.57 (0.15)	3.4
TmDHFR[c]	0.62 (80 °C)	12 (<25 °C)	0.002 (0.001) (<25 °C)	3.5
		13 (>25 °C)	1.56 (0.47) (>25 °C)	

[a] Reference 77. [b] Reference 100. [c] Reference 102. [d] Note that differences become exaggerated when k_{cat} is compared at 25 °C for the three enzymes. [e] These values are at 25 °C, with the exception of TmDHFR, which is at 40 °C.

Taken together, the results summarized in Table 4 suggest a tradeoff between protein flexibility and the efficiency of catalysis. This is particularly true for the tm-DHFR, which has a dimerization interface close to the M20 loop. Though protein dimerization is expected to increase protein stability, the resulting oligomeric structure may significantly restrict loop conformational changes required for catalysis. Analogous to the case of ht-ADH below 30 °C, the behavior of tm-DHFR below 25 °C suggests considerable rigidity that impedes the preorganization necessary to achieve the optimal alignment of substrates. The observation of $A_H/A_D \ll 1$ is most likely a reflection of an increase in a distance sampling mode required to overcome the compromised substrate geometries at the active site.

3.5.3. Psychrophilic DHFR (mp-DHFR)

As with ADH, a limited but growing body of information about psychrophilic homologues has drawn interest with respect to cold adaptations in the context of dynamics and catalysis. Recently, a psychrophilic DHFR (from *Moritella profunda*, a strict psychrophile that lives in the deep sea),

with 55% sequence identity to ec-DHFR, has been isolated and its kinetics studied.[103]

As anticipated from previous studies of psychrophilic proteins, the enzyme is thermolabile, but k_{cat} is comparable to the values observed for other DHFRs. In contrast to ec-DHFR, k_{cat}/K_m (DHF) at the physiologically relevant temperature (5 °C) is reduced 100-fold at pH 7.0, indicating loss of catalytic efficiency at reduced substrate concentrations. Analysis of the amino acid content is consistent with trends observed for other series of homologous enzymes, with a decrease in hydrophobic residues upon going from tm-DHFR to mp-DHFR. There may also be a trend[100,103] toward a lower percentage of charged residues (Lys, Arg, Glu, and Asp): tm-DHFR (28.0%), bs-DHFR (26.6%), ec-DHFR (25.8%), and mp-DHFR (22.3%). In addition, the residues glutamine and asparagine, generally regarded as thermolabile, show an increasing abundance in the psychrophile.

Although a crystal structure of the psychrophile will be required to identify specific structural implications of the above trends, the high conservation of sequence and three-dimensional structure (among three of the four DHFRs) implicates a role for differences in dynamics as a strategy used by these proteins to optimize their catalysis under different temperature environments. One interesting study, in this context, is the study of native and immobilized ec-DHFR by quasi-elastic neutron scattering; this study indicated a decrease in both the picosecond dynamics and k_{cat} for the immobilized form of the enzyme.[104]
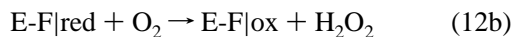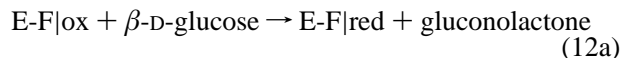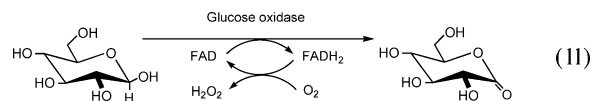
3.6. Computer Modeling of the Temperature Dependence of the Isotope Effect in DHFR

As described in section 2, the data for ADH have led to a focus on full tunneling models, as opposed to the tunneling corrections considered in earlier treatments. This approach contrasts with the work of a number of other investigators, where tunneling continues to be treated as a correction to transition state.[67−72] Extending the ensemble averaged variational transition state theory with multidimensional tunneling described in section 2, Truhlar and co-workers have come close to reproducing the temperature-independent isotope effects observed for ec-DHFR.[105] Consistent with conventional transition state theory that uses tunnel corrections, the calculations indicate that there is less tunneling at high temperatures, which would tend to lower the kinetic isotope effect. This is compensated, however, by two effects, as the temperature is elevated. First, there is an imposed trend toward a more symmetrical TS, which tends to increase the kinetic isotope effect as compensatory vibrational modes at the transition state are minimized. Second, the effective barrier at 45 °C is narrower than that at 5 °C. This increases the tunneling probability, offsetting the usual decrease associated with the tunneling correction at higher temperatures. While the resulting calculated parameters begin to approach the experimental values, there is still considerable divergence. Perhaps most importantly, it is important to question whether the methods used to reproduce the data for DHFR will be generally applicable, given the wide range of different enzyme reactions that have now been demonstrated to display largely temperature-independent isotope effects.

4. Glucose Oxidase

Glucose oxidase (GO) is a flavin-dependent enzyme that catalyzes a two-electron oxidation of β-D-glucose to its corresponding lactone, eq 11.[106] During this process, the enzyme cycles between an oxidized and reduced cofactor (eq 12a), which is returned to its oxidized state with molecular oxygen (eq 12b):

(11)

$$\text{E-F|ox} + \beta\text{-D-glucose} \rightarrow \text{E-F|red} + \text{gluconolactone}$$
(12a)

$$\text{E-F|red} + O_2 \rightarrow \text{E-F|ox} + H_2O_2 \quad (12b)$$

Given the properties of flavin cofactors, which include the capacity to undergo both one- and two-electron transfer reactions and the susceptibility of oxidized flavin to nucleophilic attack at its 4a or 5 position, a range of possible mechanisms has been proposed for the C−H activation of substrate: these include stepwise radical reactions, adduct formation between the cofactor and substrate followed by proton abstraction, and direct hydride transfer.[107]

4.1. Properties of the C–H Activation Step: Evidence for Tunneling and Its Relationship to Protein Flexibility

Analysis of the mechanism in the GO reaction has been greatly aided by the ability to remove the native flavin and reconstitute enzyme with modified cofactors of altered reduction potentials. Recent studies, that show a linear relationship between reaction driving force and rate of substrate oxidation (cf., eq 12a), indicate that a previously published rate constant for deazaflavin (a two-electron accepting flavin with properties closer to NAD$^+$) falls on a straight line with other flavin analogues.[108] This result strongly points toward a mechanism for GO that involves a formal hydride transfer from the C-1 position of substrate to cofactor. Analogous to the case of alcohol dehydrogenases, this is expected to be accompanied by prior deprotonation of the hemi-acetal at C-1, i.e., to involve hydride removal from an alcoholate intermediate.

In the course of examining rate as a function of driving force, Roth and co-workers employed the Marcus equation (eq 1) to estimate the value of λ for the enzymatic hydride transfer. Their results indicate a λ of 68 kcal/mol, which together with the estimated driving force, $\Delta G°$, leads to a free energy of activation ($\Delta G^{\ddagger}$) of ca. 15 kcal/mol.[108] A similar value for $\Delta G^{\ddagger}$ has been estimated from the temperature dependence of the reaction. This raises the question of the manner in which GO catalyzes the hydride transfer in relation to the solution reaction. The half potential for flavin reduction is not very different for free vs bound flavin enzyme, with a slightly more favorable driving force off the enzyme. Given that the solution reaction cannot be observed at 25 °C, this suggests that the reorganization energy may be even higher in solution, raising the question of how high λ can become for a hydride transfer reaction. One aspect of the difference between the reaction in solution and on the enzyme concerns the differential binding energy of glucose vs the gluconolactone, which may contribute to the driving force in a way that favors the reaction on the enzyme. For a tunneling model, the properties of the wave function overlap will also play a key role and the capacity of the enzyme to preorganize the reactants in such a way as to

facilitate this wave function overlap may contribute to catalysis in a very significant manner. This is likely to reflect an optimization of the initial donor and acceptor distance, made possible by discrete binding interactions between the enzyme and substrate, together with protein-mediated distance-sampling modes (r in Figure 7).

In actuality, finding evidence for tunneling in the GO reaction has been less than straightforward. Studies completed to date have focused on a modified substrate, 2-deoxyglucose, that permits close to full kinetic isolation of the hydrogen transfer process. Since there is no secondary hydrogen at the reactive, C-1 position of substrate, probes of tunneling have been limited to the determination of the temperature dependence of the primary kinetic isotope effect. A particular emphasis in these studies has been on the impact of modifications at the protein surface on the temperature dependence of the isotope effect. Five different isoforms were prepared through variations in the degree of protein glycosylation and via the addition of poly(ethylene glycol) (PEG) to surface lysines, with resulting molecular weights that vary from 136 to 320 kDa.[109] In addition to using 2-deoxyglucose to approximate a single rate-limiting hydrogen transfer step, a major focus was on the interpretation of the primary D/T isotope effect, since this further reduces any potential complication of kinetic complexity that can arise in H/T isotope effect measurements. As noted in early studies of GO, the magnitude of the primary H/D isotope effect is elevated to ca. 10 (ref 110) in relation to the primary hydrogen isotope effect of ca. 3.5 in alcohol dehydrogenases.[45]

The temperature dependence of the isotope effect in GO has been studied with great care, to establish the region of Arrhenius plots that represents a single rate-determining step. These indicate an A_D/A_T close to unity for both the native form of GO and a form in which surface sugars have been enzymatically removed (molecular mass for the GO of 156 and 136 kDa, respectively).[109] A value for $A_{(light)}/A_{(heavy)}$ close to one, while not allowing any conclusion about tunneling, is compatible with a full tunneling model in which $A_{(light)}/A_{(heavy)}$ can move from much greater than unity (little distance sampling) to much less than unity (a great deal of distance sampling required for efficient wave function overlap).

The intriguing aspect of this GO study comes from the characterization of the enzyme forms that have been heavily modified on their surface, with the resulting value of A_D/A_T falling to ca. 0.6 (0.08).[109] This indicates, first, that the impact of surface modification is not related to the mass of the modified protein, correcting an earlier three-point correlation.[111] Most importantly, changes in the properties of the protein at its surface are being "felt" at the enzyme active site, independent of either the nature of the modifying residue or its position. Since the modifying groups are expected to be pointing into the bulk solvent, their impact is almost certainly on the flexibility of the modified proteins. Though not yet investigated, this may be an excellent system for examining the impact of surface modification on the rate of deuterium exchange into the peptide backbone of protein.

The results for GO add to a growing list of hydride transfer enzymes in which perturbation away from the native structure leads to an increase in the observed temperature dependence of the primary hydrogen kinetic isotope effect. As summarized in Table 5, the perturbant can be site-specific mutagenesis (ec-DHFR), temperature (in the case of ht-ADH or tm-DHFR), or surface modification (GO). The aggregate

Table 5. Enzymatic Hydride Transfer Systems Where Perturbations in Enzyme Structure or Reaction Conditions Lead to a Decrease in $A_{(light)}/A_{(heavy)}$

enzyme	$A_{(light)}/A_{(heavy)}$	ref
Ht-ADH		
above 30 °C	>1	51
below 30 °C	<1	51
Ec-DHFR		
wild type	>1	77
M43W	<1	83
Tm-DHFR		
above 25 °C	~1	102
below 25 °C	<1	102
glucose oxidase		
wild type	~1	108
surface modified	<1	108

data point toward a model in which the creation of a "defect" in protein structure or flexibility impedes the ability of the enzyme to achieve an optimal preorganization of the active site (Figure 9). This places the carbon centers of the hydrogen donor and acceptor further apart than in the wild-type enzyme, increasing the need for distance sampling to effect efficient hydrogen tunneling. As introduced earlier in the context of alcohol dehydrogenases (cf. Figure 7), at nonoptimal distances, gating for the heavier nucleus (D or T) is expected to exceed that needed for efficient H transfer, raising the environmental barrier for tunneling in an isotope-dependent manner. One additional feature of the enzymes summarized in Table 5 is that the sensitivity of the temperature dependence of the isotope effect to alterations in enzyme is much more consistent than the variation in the protium rate; that is, the impact of a given perturbation on rate varies from almost unobservable to many orders of magnitude. This has led to the suggestion that the larger determinant of the observed barrier height for protium may be λ and $\Delta G°$, rather than r.[112] This aspect of the tunneling process is in need of further theoretical and experimental investigation.

4.2. Involvement of Nuclear Tunneling in the Electron Transfer Step of GO

The second half reaction of GO (eq 12b), in which O_2 is reduced to H_2O_2, has recently been shown to be limited by an outer sphere electron transfer from the reduced flavin to O_2. As in the hydride transfer reaction, the replacement of the native flavin with substituted flavins of differing driving forces has provided an estimate of λ in this half reaction, $\lambda = 24$ kcal/mol, considerably less that that measured for the hydride transfer step.[113] Upon examination of the GO active site, and by analogy to other members of this class of alcohol oxidase, a role was suggested for a protonated active site histidine 516 in reducing λ. This was confirmed by going to high pH, where H516 is deprotonated and the enzyme rate is close to the solution rate, and by mutagenesis experiments in which the histidine was replaced by alanine.[111] In both instances, λ for the oxidative half reaction increased by ca. 15 kcal/mol, thus providing very strong evidence for the role of an active site charge in reducing the outer sphere reorganization energy for electron tunneling.[114]

As discussed for electron transfer processes, the value of λ is expected to be the sum of inner and outer sphere processes, $\lambda_{tot} = \lambda_{in} + \lambda_{out}$. While changes in the protein environment are expected to be the major contributors to λ_{out}, the bond reorganizations within both O_2 and flavin will

constitute λ_{in}. In conjunction with the investigation of the impact of flavin driving force on rate, it was also possible to measure the magnitude of the oxygen-18 kinetic isotope effect upon enzymatic reduction of O_2 to the first intermediate, superoxide anion. This investigation yielded a very surprising result: in contrast to the dependence of the rate on $\Delta G°$, the value of the O-18 isotope effect was nearly constant across the series (Figure 14). Further, any effort to
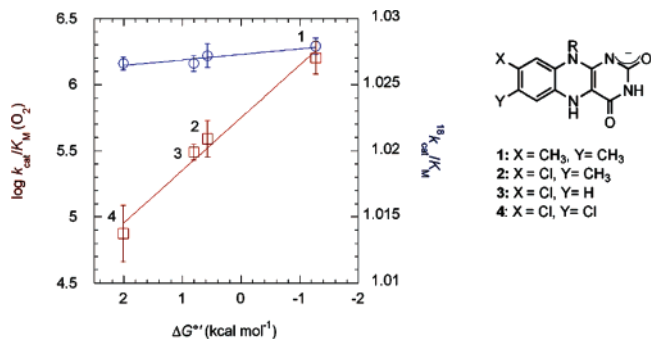

Figure 14. Driving force dependence of the observed rate $k_{cat}/K_M(O_2)$ [left ordinate and red squares] and the kinetic isotope effect $^{18}(k_{cat}/K_M(O_2))$ [right ordinate and blue circles].

model the lack of a significant trend in the O-18 isotope effect using classical Marcus theory failed.[113] This led to the recognition that the inner sphere reorganization of the O_2 molecule was likely to have a significant nuclear tunneling component. Given the high frequency for stretching of the O–O bond of O_2 (1556 cm^{-1}) in relation to the thermal energy at room temperature ($\sim$200 cm^{-1}), this conclusion is perhaps not so surprising and illustrates how the behavior of heavier nuclei such as oxygen and carbon may be much closer to the behavior of hydrogen than generally recognized.

4.3. Conformational Sampling in the Family of Alcohol Oxidases

The role of conformational sampling in the alcohol oxidase family has been addressed recently in two interesting papers, one of which presents an atomic resolution X-ray structure of cholesterol oxidase and a second which presents a single molecule kinetic study of the same enzyme. The X-ray studies of the apo-protein show two protein conformers, one of which is similar to a structure seen for an enzyme–steroid complex.[115] The structure also indicates a link between a channel to the solvent and the redox state of the cofactor. A network of residues "senses" whether the flavin is oxidized or reduced and undergoes a correlated change in motion to create a channel for O_2 binding. With regard to the hydride transfer step, the structural studies implicate a very close packing (of 3.1 Å) between the C-3 of substrate (the hydrogen donor) and the N-5 of flavin (the hydrogen acceptor).

In the single molecule kinetic studies by Xie and co-workers, the focus was on the hydride transfer step, which could be followed by the time-dependent loss in the fluorescence of the oxidized flavin.[116] The authors were able to measure the rate constant for the hydride transfer step, which was found to be variable in two distinct ways. The first involves a static disorder phenomenon that is proposed to arise from protein defects arising during protein purification and storage. The second type of disorder (dynamic) appears to be more directly relevant to catalysis, involving

a relatively slow transition between enzyme forms that are characterized by different rate constants for the hydride transfer step. This latter observation supports the view that any given protein will experience a very large number of conformations that differ in their catalytic competence. Although the design of these single molecule experiments was limited to the detection of conformational sampling slower than the hydride transfer step, the results from such studies can serve as a "beacon" for the expected, extensive, and fairly rapid interconversion among multiple protein conformations that vary in their catalytic efficiencies.

5. Concluding Remarks

At this juncture it is widely accepted that hydrogen tunneling occurs in C–H activation reactions in general and for hydride transfer reactions in particular. In recent years, the question has been raised whether hydrogen tunneling occurs more often in an enzyme-catalyzed reaction than for a comparable reaction in solution. There are two primary routes to address this question. The first is to compare the enzyme-catalyzed process to the solution reaction. The second strategy is to mutate an enzyme such that the hydrogen transfer process is modified, allowing a comparison of the tunneling properties in the mutant to those in the wild-type enzyme.

As summarized in this review, there are now numerous examples of the use of site-specific mutagenesis in hydride transfer reactions, with the repeated observation of changes for the mutated enzyme that include an increase in the temperature dependence of the kinetic isotope effect (Table 5) and a decrease in the aberrant nature of the Swain–Schaad relationship for the mutant form of the enzyme (Table 1). The implications of these findings are presented in section 2.3 and will be summarized below. Fewer studies are available that involve the comparison of a model reaction to the enzyme-catalyzed counterpart, in large part, because of the difficulty in establishing a model reaction that provides a precise mimic of the enzyme reaction. To date, however, several models have been reported for a B-12-dependent hydrogen atom abstraction,[117] a ferric hydroxide-catalyzed oxidation of fatty acids,[118] and the isomerization of a β–γ unsaturated keto-steroid to the conjugated α–β product via a proton abstraction.[119] In the first case, Finke and co-workers concluded that the temperature dependence of the kinetic isotope effect was similar for both the enzyme-catalyzed and model reactions,[117] whereas in the keto-steroid isomerase reaction, the breakdown of the Swain–Schaad relationship for the secondary isotope effect was concluded to be greater for the enzyme reaction.[119] Further, comparison of a model reaction for the iron-catalyzed oxidation of a fatty acid substrate[118] indicates a hugely reduced isotope effect relative to the case of the enzymatic reaction.[4] In a very recent approach, Tanizawa and co-workers[120] removed the catalytic base from the active site of a copper amine oxidase, reducing the enzyme activity by ca. 10^6. This "base-free enzyme", which can be considered a reasonable model for the noncatalyzed reaction, revealed a substantially larger temperature dependence for the primary isotope effect than was seen for the wild-type enzyme.[120] In the majority of instances studied thus far, different tunneling parameters are being observed in the model and enzyme reactions.

With the demonstrations of extensive tunneling and the elaboration of a full tunneling model (cf. section 2.3), the

more reasonable question to address is "what is the impact of the enzyme active site on the properties of tunneling" rather than "to what extent does the enzyme increase the degree of tunneling." We note that while variational transition state theory (VTST) is essentially a tunnel correction model that differs significantly from the full tunneling model advanced in this review, it does incorporate many of the same themes in its analysis of the role of tunneling in enzyme reactions; these include multidimensionality, changes in barrier shape, and the coupling of protein motion to quantum mechanical tunneling. It has been reported that VTST can approximate the temperature independence of the isotope effect for the wild-type ec-DHFR reaction, by incorporating a narrowing of the reaction barrier shape with increasing temperature,[105] a phenomenon similar to the proposed behavior of the ht-ADH above 30 °C (cf. section 2.3.2 and below). At the current time, however, it appears unlikely that the theoretical basis of VTST will be able to be generalized to the wide variety of mechanistically different enzyme-catalyzed C−H abstraction reactions studied. The full tunneling model, advanced herein, provides a clear context for our understanding of either temperature-independent or -dependent primary kinetic isotope effects.

Inherent in a full tunneling model is the link of motions within the environment to the tunneling probability. Detecting and characterizing these motions has taken on increasing importance in our effort to understand the origins of enzyme catalysis. It is generally accepted that the protein is constantly interconverting among numerous configurations on time scales that vary from milliseconds to picoseconds. Motions that have been detected via single molecule studies of enzyme reactions indicate different protein conformers with altered catalytic properties. As noted earlier in the discussion of cholesterol oxidase (cf. section 4.3), the nature of the available single molecule experiments dictates that only motions that are slower than or comparable to catalysis can be detected, since motions that are faster than catalysis will show averaged properties and not be distinguishable.

The properties of the kinetic isotope effects observed in enzymatic hydride transfer reactions provide powerful tools in our efforts to describe and distinguish the millisecond to picosecond motions that are linked to the C−H activation step. The alcohol dehydrogenase from the thermophilic organism *B. stearothermophilus* (ht-ADH) has offered a unique opportunity to monitor and compare the properties of chemical and protein dynamics above and below a transition at 30 °C. A remarkable observation has been that a specific and local region within the substrate binding domain undergoes an increase in flexibility that correlates with a decrease in the enthalpy of activation, a less temperature-dependent isotope effect, and a more aberrant Swain−Schaad relationship (Table 3). Since the latter two parameters implicate a more structured active site (cf. Figure 8), it has become necessary to parse the protein motions into two categories of motion, termed the preorganization and reorganization terms (Figure 9). The former, which can be categorized as a "coarse tuning", involves the rapid sampling of a large number of configurations with only a very small fraction of these expected to reach the precise alignment of essential components within the active site that is necessary to support tunneling. This family of possible conformers can be treated in a statistical manner, with the observed rate constant representing the fraction of functional conformers [$f(i)$] multiplied by the rate constants for H-tunneling within these conformers [$k(i)$]:

$$k_{obs} = \sum_i f(i)\, k(i) \tag{13}$$

It should be noted that these motions are likely to be both proximal and distal to the active site and to take place via a wide range of motions (nanosecond to millisecond). These motions may not be visible in X-ray structures of proteins, which generally depict a single or small number of possible conformations (cf. ref 121).

The second category of motion, the reorganization or "fine tuning", is derived from a modified Marcus theory in which the activation energy represents the barrier to achieve both a transient degeneracy between the reactant and product states, and the appropriate distance (r_x) between the H-donor and acceptor atoms (Figure 7). It is the latter term that primarily determines the temperature dependence of the kinetic isotope effect, while both terms determine the rate of protium transfer to varying degrees depending on the enzyme in question. These motions may be expected to be more proximal to the reacting center and to occur on nanosecond to picosecond time scales.

An "optimized active site" may, in fact, be expected to be less dynamical in its reorganization properties. Figure 8 shows how optimized active sites may affect inner sphere reorganization, inflating the Swain−Schaad relationship for secondary kinetic isotope effects. Release of these constraints upon loosening of the active site (by a change in temperature or site-specific mutagenesis) leads to "a more normal" Swain−Schaad parameter (Tables 1 and 3) and generally more temperature-dependent isotope effects (Tables 3 and 5). It is of interest that the dynamics maintained at the active site may be quite different from the dynamics elsewhere in the protein. *In the case of ht-ADH, the active site is apparently able to become more constrained at high temperature, as the overall flexibility of the protein increases!*

In conclusion, this review has sought to illuminate what has been learned recently about enzymatic catalysis in the context of hydride transfer. This follows upon decades of research that have yielded a well-established arsenal of means by which enzymes can catalyze reactions, including acid−base catalysis, hydrogen bonding, electrostatics, and entropic effects,[6,122] with the most current work focusing on the consequences of setting these contributions into motion. While the importance of tunneling and dynamics was essentially assumed in this review, it is only in the last 5 years that the field of enzymology has seen a rapid convergence around this idea. A large number of research groups studying a variety of enzymes that catalyze hydrogen transfer, many of which are not reviewed here, have begun to settle on unifying themes. Increasing crosstalk between theoretical, computational, and experimental chemists has begun to yield significant dividends. Theoretical approaches offer the opportunity to probe phenomena that cannot be easily explored experimentally and, in the ideal situations, provide a starting point for the generation of new, experimentally testable hypotheses. As computational power permits longer simulations and as experimental methods are refined to higher time and spatial resolution, a generalized theory for hydrogen transfer that can describe and predict the properties of enzymatic hydride transfer is becoming a feasible reality.

6. Acknowledgment

7. References

(1) Wolfenden, R.; Snider, M. J. *Acc. Chem. Res.* **2001**, *34*, 938.
(2) Bell, R. P. In *The Tunnel Effect in Chemistry*; Chapman and Hall: New York, 1980.
(3) Klinman, J. P. *Proc. R. Soc. London*, in preparation.
(4) Knapp, M. J.; Rickert, K.; Klinman, J. P. *J. Am. Chem. Soc.* **2002**, *124*, 3865.
(5) Pauling, L. *Chem. Eng. News* **1946**, *24*, 1375.
(6) Jencks, W. P. In *Catalysis in Chemistry and Enzymology*; McGraw-Hill: New York, 1969.
(7) Karplus, M.; Kuriyan, J. *Proc. Natl. Acad. Sci., U.S.A.* **2005**, *102*, 6679.
(8) Doring, K.; Surrey, T.; Nollert, P.; Jahnig, F. *Eur. J. Biochem.* **1999**, *266*, 477.
(9) Karplus, M.; Gao, Y. Q.; Ma, J. P.; Van der Vaart, A.; Yang, W. *Philos. Trans. R. Soc. London, Ser. A* **2005**, *363*, 331.
(10) Sparrer, H.; Lilie, H.; Buchner, J. *J. Mol. Biol.* **1996**, *258*, 74.
(11) Bolton, W.; Perutz, M. F. *Nature* **1970**, *228*, 551.
(12) McCammon, J.; Harvey, S. In *Dynamics of Proteins and Nucleic Acids*; Press Syndicate of the University of Cambridge: New York, 1987; p 234.
(13) Mincer, J. S.; Schwartz, S. D. *J. Chem. Phys.* **2004**, *120*, 7755.
(14) Palczewski, K.; Kumasaka, T.; Hori, T.; Behnke, C. A.; Motoshima, H.; Fox, B. A.; Le Trong, I.; Teller, D. C.; Okada, T.; Stenkamp, R. E.; Yamamoto, M.; Miyano, M. *Science* **2000**, *289*, 739.
(15) Kim, J. E.; Pan, D. H.; Mathies, R. A. *Biochemistry* **2003**, *42*, 5169.
(16) Kukura, P.; McCamant, D. W.; Yoon, S.; Wandschneider, D. B.; Mathies, R. A. *Science* **2005**, *310*, 1006.
(17) Bustamante, C.; Keller, D.; Oster, G. *Acc. Chem. Res.* **2001**, *34*, 412.
(18) Dodd, J. A.; Brauman, J. I. *J. Am. Chem. Soc.* **1984**, *106*, 5356.
(19) Marcus, R. A.; Sutin, N. *Biochim. Biophys. Acta* **1985**, *811*, 265.
(20) Warshel, A. *J. Biol. Chem.* **1998**, *273*, 27035.
(21) Hur, S.; Bruice, T. C. *Proc. Natl. Acad. Sci., U.S.A.* **2003**, *100*, 12015.
(22) Kiefer, P. M.; Hynes, J. T. *J. Phys. Chem. A* **2004**, *108*, 11793.
(23) Bahnson, B. J.; Klinman, J. P. *Methods Enzymol.* **1995**, *249*, 374.
(24) Kohen, A.; Klinman, J. P. *Acc. Chem. Res.* **1998**, *31*, 397.
(25) Kohen, A.; Klinman, J. P. In *Chemistry and Biology*; Schreiber, S. L., Nicolaou, K. C., Eds.; Elsevier Science, Ltd: London, U.K., 1999; Vol. 6, pp R191−404.
(26) Hammes-Schiffer, S. *Biochemistry* **2002**, *41*, 13335.
(27) Heyes, D. J.; Hunter, C. N.; van Stokkum, I. H. M.; van Grondelle, R.; Groot, M. L. *Nat. Struct. Biol.* **2003**, *10*, 491.
(28) Dickinson, F. M.; Dalziel, K. *Biochem. J.* **1967**, *104*, 165.
(29) Dickinson, F. M.; Dalziel, K. *Nature* **1967**, *214*, 31.
(30) Rossman, M. G.; Liljas, A.; Branden, C.-I.; Banaszak, L. J. In *The Enzymes*, 3rd ed.; Academic Press: New York, 1970; Vol. IX, p 61.
(31) Kovaleva, E. G.; Plapp, B. V. *Biochemistry* **2005**, *44*, 12797.
(32) Bush, K.; Shiner, V. J.; Mahler, H. R. *Biochemistry* **1973**, *12*, 4802.
(33) Klinman, J. P. *J. Biol. Chem.* **1972**, *247*, 7977.
(34) Klinman, J. P. *Biochemistry* **1976**, *15*, 2018.
(35) Bahnson, B. J.; Colby, T. D.; Chin, J. K.; Goldstein, B. M.; Klinman, J. P. *Proc. Natl. Acad. Sci., U.S.A.* **1997**, *94*, 12797.
(36) Hermes, J. D.; Cleland, W. W. *J. Am. Chem. Soc.* **1984**, *106*, 7263.
(37) Welsh, K. M.; Creighton, D. J.; Klinman, J. P. *Biochemistry* **1980**, *19*, 2005.
(38) Cha, Y.; Murray, C. J.; Klinman, J. P. *Science* **1989**, *243*, 1325.
(39) Swain, C. G.; Stivers, E. C.; Reuwer, J. F.; Schaad, L. J. *J. Am. Chem. Soc.* **1958**, *80*, 5885.
(40) Kohen, A.; Jensen, J. H. *J. Am. Chem. Soc.* **2002**, *124*, 3858.
(41) Hirschi, J.; Singleton, D. A. *J. Am. Chem. Soc.* **2005**, *127*, 3294.
(42) Saunders, W. H. *J. Am. Chem. Soc.* **1985**, *107*, 164.
(43) Huskey, W. P.; Schowen, R. L. *J. Am. Chem. Soc.* **1983**, *105*, 5704.
(44) Bahnson, B. J.; Park, D. H.; Kim, K.; Plapp, B. V.; Klinman, J. P. *Biochemistry* **1993**, *32*, 5503.
(45) Rubach, J. K.; Plapp, B. V. *Biochemistry* **2003**, *42*, 2907.
(46) Tsai, S. C.; Klinman, J. P. *Biochemistry* **2001**, *40*, 2303.
(47) Karlsson, A.; El-Ahmad, M.; Johansson, K.; Shafqat, J.; Jornvall, H.; Eklund, H.; Ramaswamy, S. *Chemico-Biol. Int.* **2003**, *143*, 239.
(48) Korkhin, Y.; Kalb, A. J.; Peretz, M.; Bogin, O.; Burstein, Y.; Frolow, E. *Protein Sci.* **1999**, *8*, 1241.
(49) Ceccarelli, C.; Liang, Z.-X.; Strickler, M.; Prehna, G.; Goldstein, B. M.; Klinman, J. P.; Bahnson, B. J. *Biochemistry* **2004**, *43*, 5266.
(50) Papanikolau, Y.; Tsigos, I.; Papadovasilaki, M.; Bouriotis, V.; Petratos, K. *Acta Crystallogr., Sect. F: Struct. Biol. Cryst. Commun.* **2005**, *61*, 246.
(51) Kohen, A.; Cannio, R.; Bartolucci, S.; Klinman, J. P. *Nature* **1999**, *399*, 496.
(52) Meyer, M. P.; Klinman, J. P. *Chem. Phys.* **2005**, *319*, 283.
(53) Basran, J.; Patel, S.; Sutcliffe, M. J.; Scrutton, N. S. *J. Biol. Chem.* **2001**, *276*, 6234.
(54) Kohen, A.; Klinman, J. P. *J. Am. Chem. Soc.* **2000**, *122*, 10738.
(55) Liang, Z. X.; Lee, T.; Resing, K. A.; Ahn, N. G.; Klinman, J. P. *Proc. Natl. Acad. Sci., U.S.A.* **2004**, *101*, 9556.
(56) Hvidt, A.; Nielsen, S. O. *Adv. Protein Chem.* **1966**, *21*, 287.
(57) Maity, H.; Lim, W. K.; Rumbley, J. N.; Englander, S. W. *Science* **2003**, *12*, 153.
(58) Bai, Y. W.; Sosnick, T. R.; Mayne, L.; Englander, S. *Science* **1995**, *269*, 192.
(59) Liang, Z. X.; Tsigos, I.; Lee, T.; Bouriotis, V.; Resing, K. A.; Ahn, N. G.; Klinman, J. P. *Biochemistry* **2004**, *43*, 14676.
(60) Liang, Z. X.; Tsigos, I.; Bouriotis, V.; Klinman, J. P. *J. Am. Chem. Soc.* **2004**, *126*, 9500.
(61) Liang, Z. X.; Klinman, J. P. Unpublished data.
(62) Fields, P. A.; Somero, G. N. *Proc. Natl. Acad. Sci., U.S.A.* **1998**, *95*, 11476.
(63) Holland, L. Z.; McFall-Ngai, M.; Somero, G. N. *Biochemistry* **1997**, *36*, 3207.
(64) Fields, P. A.; Wahlstrand, B. D.; Somero, G. N. *Eur. J. Biochem.* **2001**, *268*, 4497.
(65) Fields, P. A.; Kim, Y. S.; Carpenter, J. F.; Somero, G. N. *J. Exptl. Biol.* **2002**, *205*, 1293.
(66) Rucker, J.; Klinman, J. P. *J. Am. Chem. Soc.* **1999**, *121*, 1997.
(67) Skodje, R. T.; Truhlar, D. G.; Garrett, B. C. *J. Chem. Phys.* **1982**, *77*, 5955.
(68) Fernandez-Ramos, A.; Truhlar, D. G. *J. Chem. Phys.* **2001**, *114*, 1491.
(69) Alhambra, C.; Corchado, J. C.; Sanchez, M. L.; Gao, J. L.; Truhlar, D. G. *J. Am. Chem. Soc.* **2000**, *122*, 8197.
(70) Alhambra, C.; Corchado, J.; Sanchez, M. L.; Garcia-Viloca, M.; Gao, J.; Truhlar, D. G. *J. Phys. Chem. B* **2001**, *105*, 11326.
(71) Truhlar, D. G.; Gao, J. L.; Garcia-Viloca, M.; Alhambra, C.; Corchado, J.; Sanchez, M. L.; Poulsen, T. D. *Int. J. Quantum Chem.* **2004**, *100*, 1136.
(72) Cui, Q.; Elstner, M.; Karplus, M. *J. Phys. Chem. B* **2002**, *106*, 2721.
(73) Almarsson, O.; Karaman, R.; Bruice, T. C. *J. Am. Chem. Soc.* **1992**, *114*, 8702.
(74) Luo, J.; Bruice, T. C. *Proc. Natl. Acad. Sci., U.S.A.* **2004**, *101*, 13152.
(75) Caratzoulas, S.; Mincer, J. S.; Schwartz, S. D. *J. Am. Chem. Soc.* **2002**, *124*, 3270.
(76) Mincer, J. S.; Schwartz, S. D. *J. Phys. Chem. B* **2003**, *107*, 366.
(77) Sikorski, R. S.; Wang, L.; Markham, K. A.; Rajagopalan, P. T. R.; Benkovic, S. J.; Kohen, A. *J. Am. Chem. Soc.* **2004**, *126*, 4778.
(78) Francisco, W. A.; Knapp, M. J.; Blackburn, N. J.; Klinman, J. P. *J. Am. Chem. Soc.* **2002**, *124*, 8194.
(79) Basran, J.; Sutcliffe, M. J.; Scrutton, N. S. *Biochemistry* **1999**, *38*, 3218.
(80) Basran, J.; Sutcliffe, M. J.; Scrutton, N. S. *J. Biol. Chem.* **2001**, *276*, 24581.
(81) Harris, R. J.; Meskys, R.; Sutcliffe, M. J.; Scrutton, N. S. *Biochemistry* **2000**, *39*, 1189.
(82) Abad, J. L.; Camps, F.; Fabrias, G. *Angew. Chem., Int. Ed.* **2000**, *39*, 3279.
(83) Wang, L.; Goodey, N. M.; Benkovic, S. J.; Kohen, A. *Proc. R. Soc. London*, in preparation.
(84) Fierke, C. A.; Johnson, K. A.; Benkovic, S. J. *Biochemistry* **1987**, *26*, 4085.
(85) Williams, J. W.; Morrison, J. F.; Duggleby, R. G. *Biochemistry* **1979**, *18*, 2567.
(86) Sawaya, M. R.; Kraut, J. *Biochemistry* **1997**, *36*, 586.
(87) Schnell, J. R.; Dyson, H. J.; Wright, P. E. *Annu. Rev. Biophys. Biomol. Struct.* **2004**, *33*, 119.
(88) Epstein, D. M.; Benkovic, S. J.; Wright, P. E. *Biochemistry* **1995**, *34*, 11037.
(89) McElheny, D.; Schnell, J. R.; Lansing, J. C.; Dyson, H. J.; Wright, P. E. *Proc. Natl. Acad. Sci., U.S.A.* **2005**, *102*, 5032.
(90) Schnell, J. R.; Dyson, H. J.; Wright, P. E. *Biochemistry* **2004**, *43*, 374.
(91) Agarwal, P. K.; Billeter, S. R.; Rajagopalan, P. T. R.; Benkovic, S. J.; Hammes-Schiffer, S. *Proc. Natl. Acad. Sci., U.S.A.* **2002**, *99*, 2794.
(92) Li, L. Y.; Falzone, C. J.; Wright, P. E.; Benkovic, S. J. *Biochemistry* **1992**, *31*, 7826.
(93) Mildvan, A. S.; Weber, D. J.; Kuliopulos, A. *Arch. Biochem. Biophys.* **1992**, *294*, 327.
(94) Kraut, D. A.; Carroll, K. S.; Herschlag, D. *Annu. Rev. Biochem.* **2003**, *72*, 517.
(95) Wong, K. F.; Selzer, T.; Benkovic, S. J.; Hammes-Schiffer, S. *Proc. Natl. Acad. Sci., U.S.A.* **2005**, *102*, 6807.

(96) Rajagopalan, P. T. R.; Zhang, Z. Q.; McCourt, L.; Dwyer, M.; Benkovic, S. J.; Hammes, G. G. *Proc. Natl. Acad. Sci., U.S.A.* **2002**, *99*, 13481.

(97) Zhang, Z. Q.; Rajagopalan, P. T. R.; Selzer, T.; Benkovic, S. J.; Hammes, G. G. *Proc. Natl. Acad. Sci., U.S.A.* **2004**, *101*, 2764.

(98) Hammes-Schiffer, S.; Benkovic, S. J. *Annu. Rev. Biochem.* **2006**, *75*, 519.

(99) Northrop, D. B. *Biochemistry* **1975**, *14*, 2644.

(100) Kim, H. S.; Damo, S. M.; Lee, S. Y.; Wemmer, D. E.; Klinman, J. P. *Biochemistry* **2005**, *44*, 11428.

(101) Wolf-Watz, M.; Thai, V.; Henzler-Wildman, K.; Hadjipavlou, G.; Eisenmesser, E. Z.; Kern, D. *Nat. Struct. Mol. Biol.* **2004**, *11*, 945.

(102) Maglia, G.; Allemann, R. K. *J. Am. Chem. Soc.* **2003**, *125*, 13372.

(103) Xu, Y.; Feller, G.; Gerday, C.; Glansdorff, N. *J. Bacteriol.* **2003**, *185*, 5519.

(104) Tehei, M.; Smith, J. C.; Monk, C.; Ollivier, J.; Oetti, M.; Kurkal, V.; Daniel, R. M. *Biophys. J.* **2006**, *90*, 1090.

(105) Pu, J. Z.; Ma, S. H.; Gao, J. L.; Truhlar, D. G. *J. Phys. Chem. B* **2005**, *109*, 8551.

(106) Gibson, Q. H.; Massey, V.; Swoboda, B. E. P. *J. Biol. Chem.* **1964**, *239*, 3927.

(107) Walsh, C. In *Enzymatic Reaction Mechanisms*; W. H. Freeman: San Francisco, CA, 1979; pp 358−405.

(108) Brinkley, D. W.; Roth, J. P. *J. Am. Chem. Soc.* **2005**, *127*, 15720.

(109) Seymour, S. L.; Klinman, J. P. *Biochemistry* **2002**, *41*, 8747.

(110) Kohen, A.; Jonsson, T.; Klinman, J. P. In *Techniques in Protein Chemistry*; Marshak, D. R., Ed.; Academic Press: New York, 1997; pp 311−319.

(111) Kohen, A.; Jonsson, T.; Klinman, J. P. *Biochemistry* **1997**, *36*, 2603.

(112) Klinman, J. P. *Biochim. Biophys. Acta*, in press.

(113) Roth, J. P.; Wincek, R.; Nodet, G.; Edmondson, D. E.; McIntire, W. S.; Klinman, J. P. *J. Am. Chem. Soc.* **2004**, *126*, 15120.

(114) Roth, J. P.; Klinman, J. P. *Proc. Natl. Acad. Sci., U.S.A.* **2003**, *100*, 62.

(115) Lario, P. I.; Sampson, N.; Vrielink, A. *J. Mol. Biol.* **2003**, *326*, 1635.

(116) Lu, H. P.; Xun, L. Y.; Xie, X. S. *Science* **1998**, *282*, 1877.

(117) Doll, K. M.; Bender, B. R.; Finke, R. G. *J. Am. Chem. Soc.* **2003**, *125*, 10877.

(118) Goldsmith, C. R.; Jonas, R. T.; Stack, T. D. P. *J. Am. Chem. Soc.* **2002**, *124*, 83.

(119) Wilde, T. C.; Blotny, G.; Pollack, R. M. Unpublished results.

(120) Murakawa, T.; Okajima, T.; Kuroda, S.; Nakamoto, T.; Taki, M.; Yamamoto, Y.; Hayashi, H.; Tanizawa, K. *Biochem. Biophys. Res. Commun.* **2006**, *342*, 414.

(121) Masgrau, L.; Roujeinikova, A.; Johannissen, L. O.; Hothi, P.; Basran, J.; Ranaghan, K. E.; Mulholland, A. J.; Suctliffe, M. J.; Scrutton, N. S.; Leys, D. *Science* **2006**, *312*, 237.

(122) Jencks, W. P. *Adv. Enzymol. Relat. Areas Mol. Biol.* **1975**, *43*, 219.

(123) Rucker, J.; Cha, Y.; Jonsson, T.; Grant, K. L.; Klinman, J. P. *Biochemistry* **1992**, *31*, 11489.

(124) Schneider, M. E.; Stern, M. J. *J. Am. Chem. Soc.* **1972**, *94*, 1517.

(125) Rajagopalan, P. T. R.; Lutz, S.; Benkovic, S. J. *Biochemistry* **2002**, *41*, 12618.

(126) Antoniou, D.; Basner, J.; Núñez, S.; Schwartz, S. D. *Chem. Rev.* **2006**, *106*, pp 3170−3187, http://dx.doi.org/10.1021/cr0503052.